Optical Characterization of Molten Fluoride Systems for FHR Applications

Will Derdeyn

Advisor: Mark Anderson

Personal Background

- Born and raised in St. Louis, MO
- Dartmouth college in Hanover, NH
- Abengoa Bioenergy in Hugoton, KS

- Music: Kurt Vile, The War on Drugs
- Comedy: Tim Robinson, Tim Heidecker

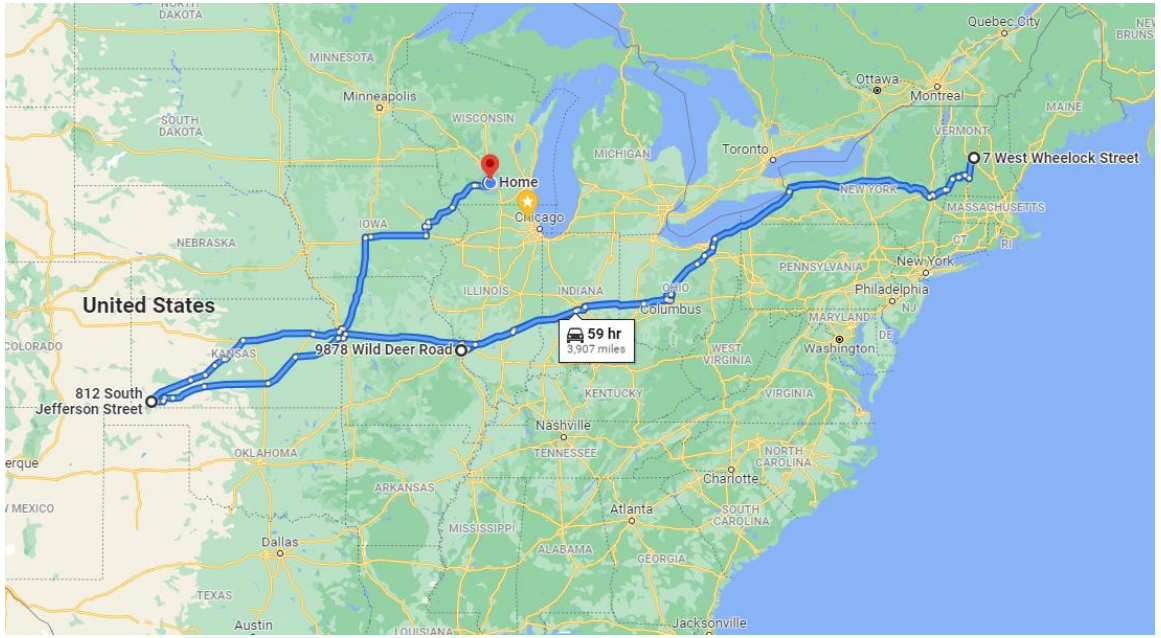

FHR Technology

- Fluoride salt-cooled high temperature reactors (FHRs) are a sub-class of molten salt reactors (MSRs) Gen IV design
- $LiF\text{-}BeF_2$ (34-66 mol%) or FLiBe is the primary coolant
- Graphite pebbles (3 cm diameter) float in the coolant and contain dispersed TRISO fuel particles

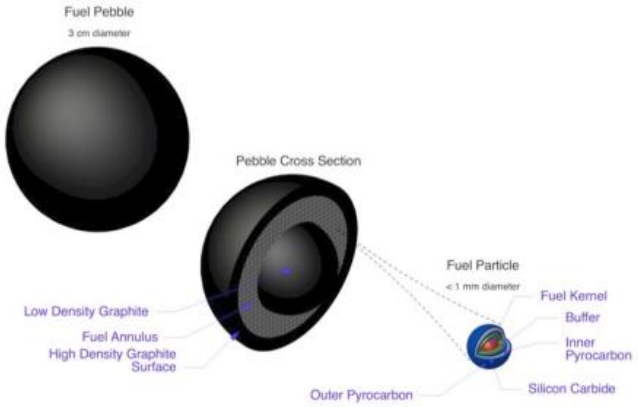

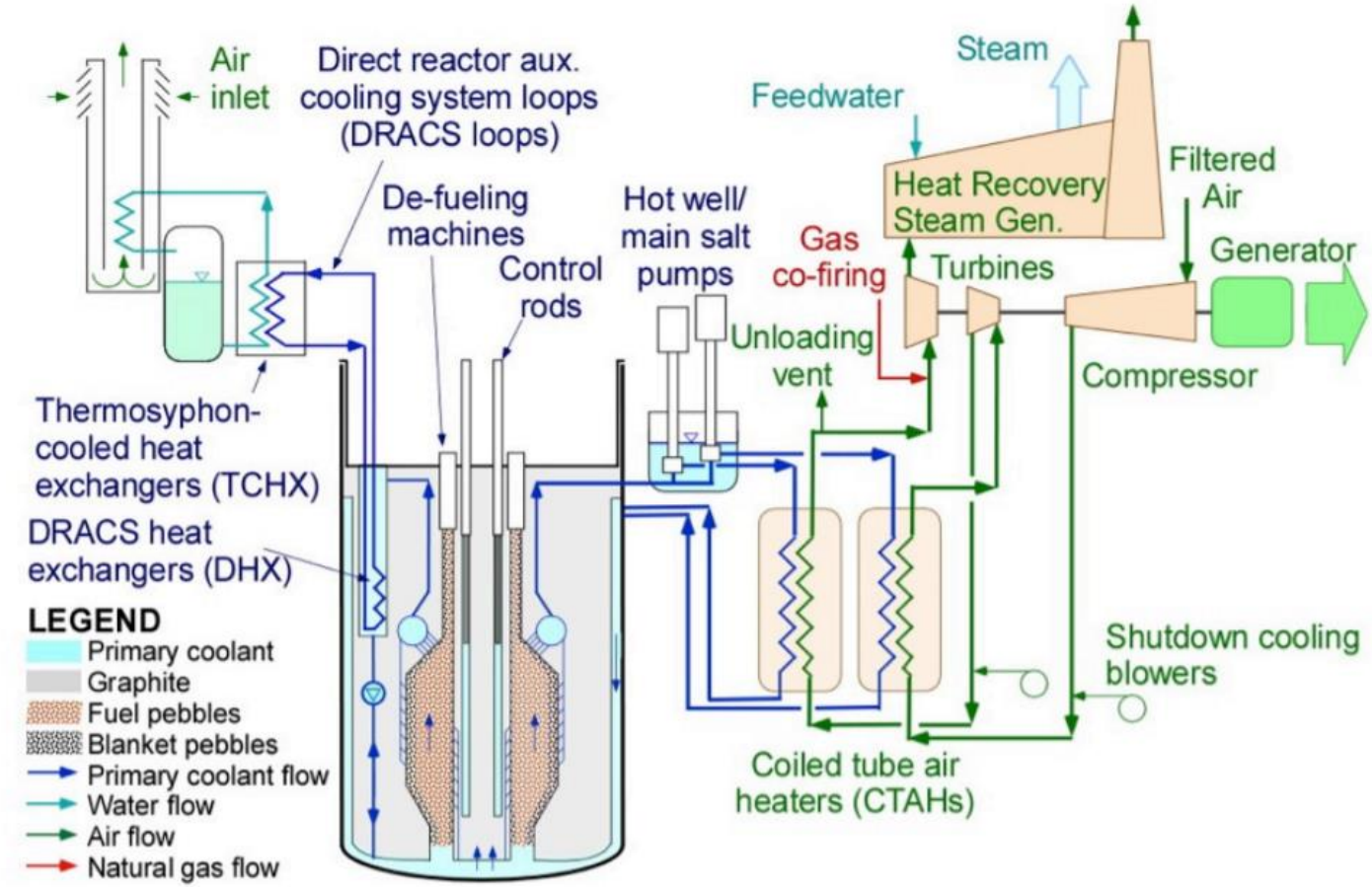

Radiative Heat Transfer (RHT) in FLiBe [1]

- CFD simulation of FLiBe flowing in 2 cm-diameter tube under forced convection at wall temperature of 700 °C

- Gray absorption coefficient: κ
- Pipe diameter: s
- Gray optical thickness: $\tau = \kappa s$

- For large ($\tau > 70$) or small ($\tau < 0.06$) τ, RHT will have negligible impact and the melt is considered either opaque or transparent
- Within the intermediate region, RHT impacts can be relatively large, and there is strong sensitivity to wall emissivity

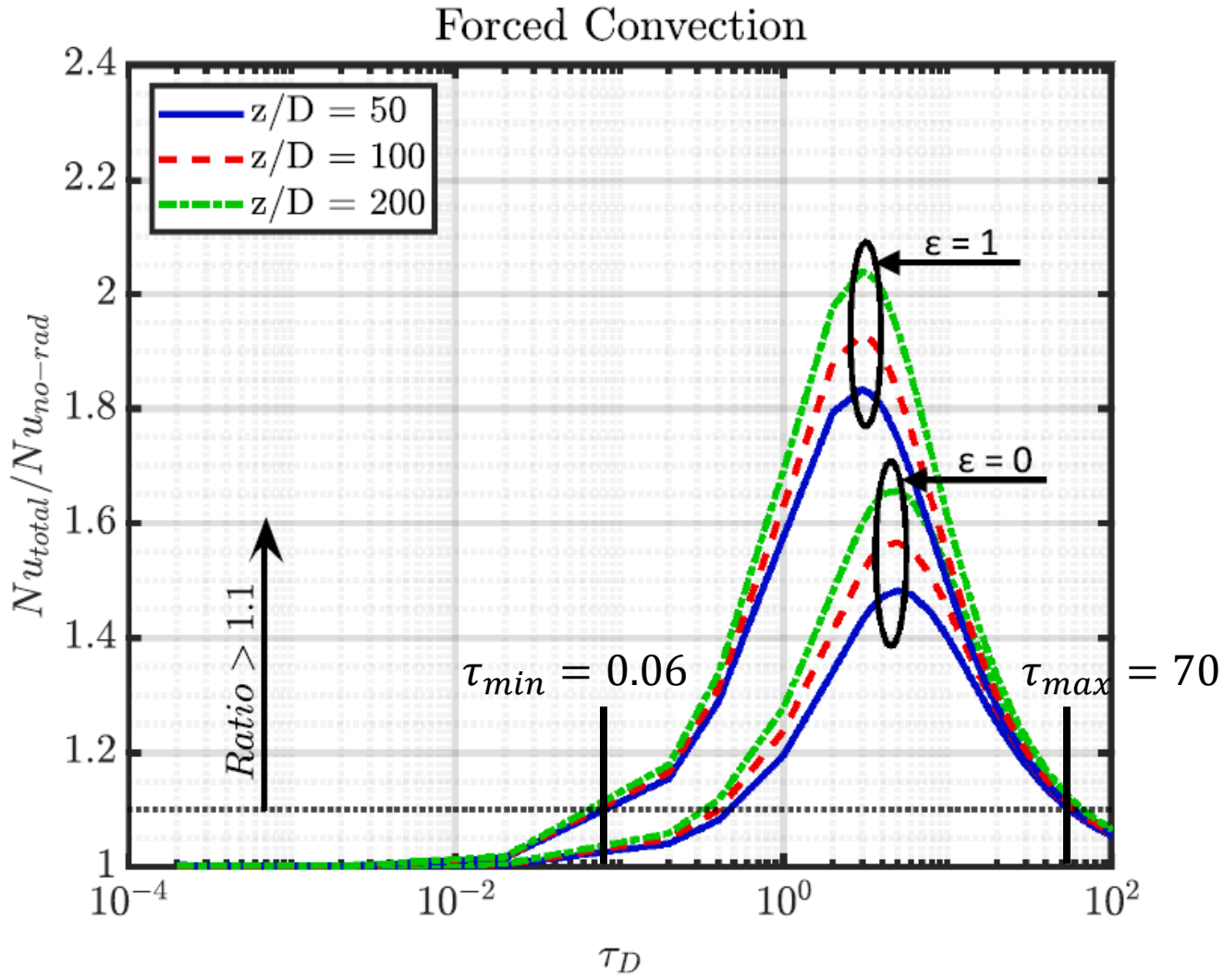

[1] M. Abou Dbai, R. O. Scarlat, et al., 'Radiative heat transfer in FLiBe molten salt participating medium in a vertical heated tube under forced and mixed convection laminar flows', Nucl. Eng. Des., vol. 368, no. July, p. 110775, (2020).

FLiBe Optical Thickness

- Given FLiBe's predicted κ_λ [2] and a fixed value for s, τ_λ can be calculated and compared with the Planck distribution (T = 700 °C)
- Using the gray τ range of maximal RHT impact, wavelength ranges of interest can be generated as a function of s
- The wavelength range of maximal RHT impact overlaps with substantial blackbody intensity, indicating that RHT impact is expected

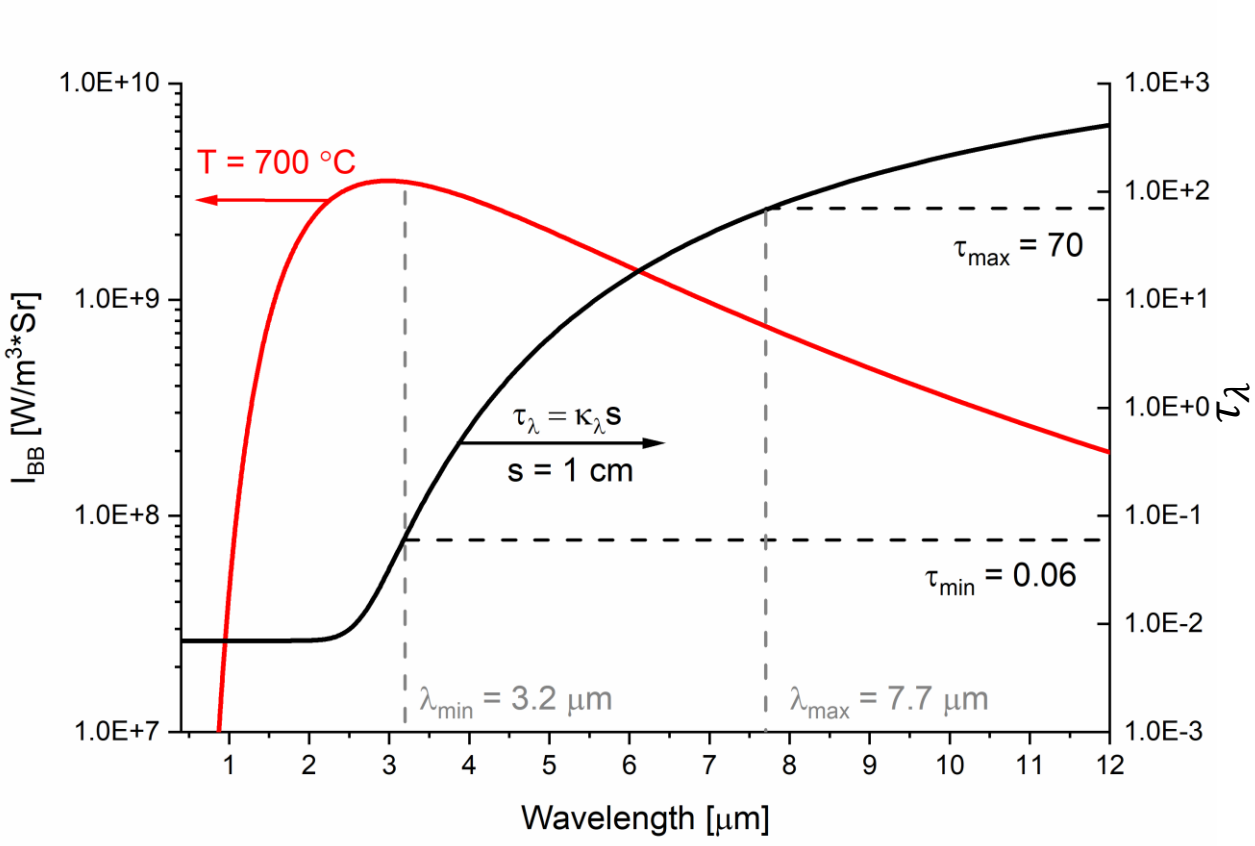

*[2] S. Liu, T. Su, et al., 'Investigation on molecular structure of molten Li2BeF4(FLiBe) salt by infrared absorption spectra and density functional theory (DFT)', J. Mol. Liq., **vol. 242**, pp. 1052–1057, (2017).*

Research question: What is the expected emissivity of SS316 salt-facing heat exchanger surfaces in a FLiBe-cooled reactor?

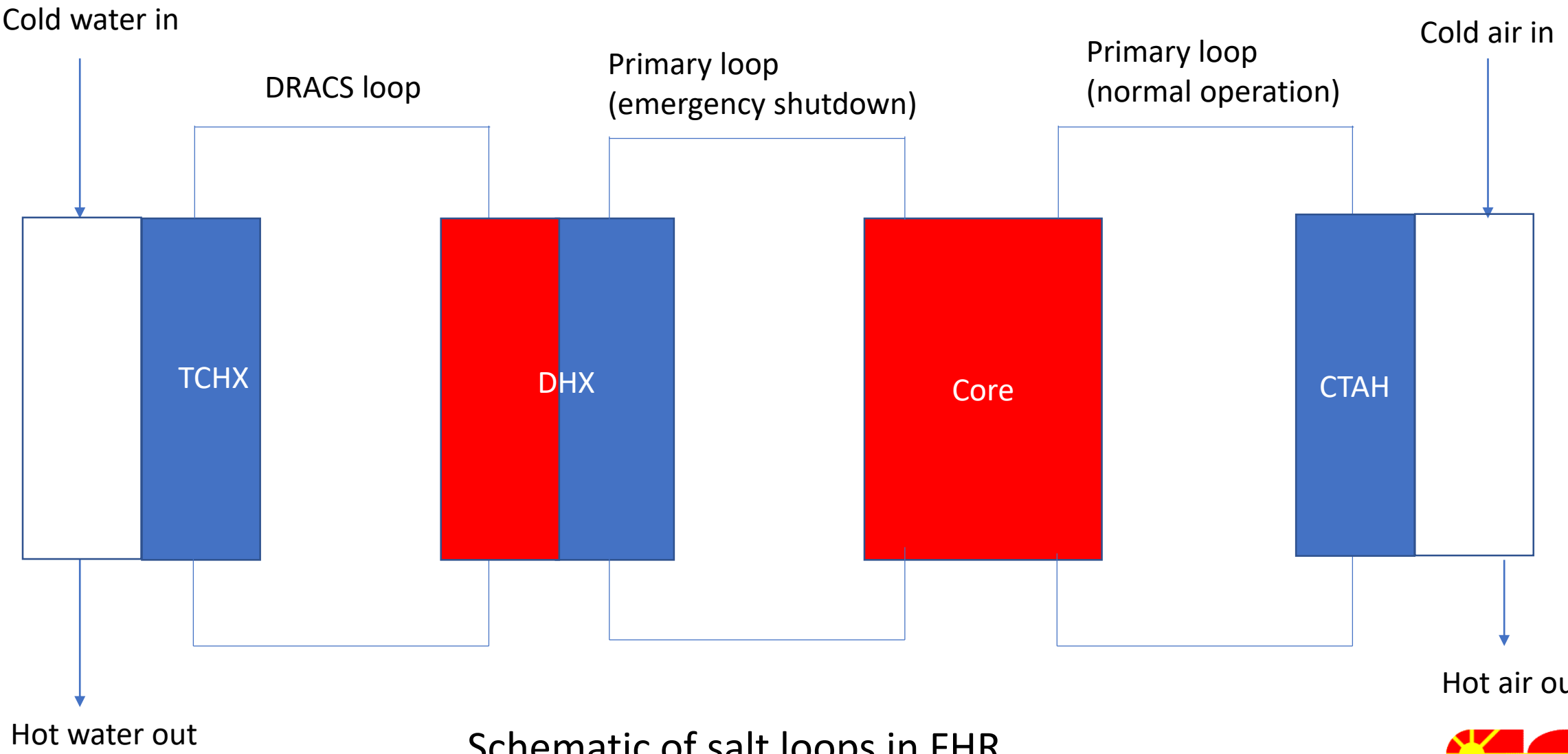

Schematic of salt loops in FHR

Exposure of SS316 to flowing FLiBe

- 2 gpm flow rate
- 2 m/s test section velocity
- 1000 hours
- 2 coupons: 1.5 x 2 x 0.1 cm

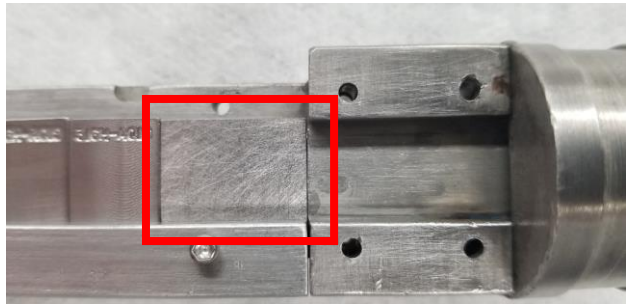

Hot leg: 700 °C

Cold leg: 650 °C

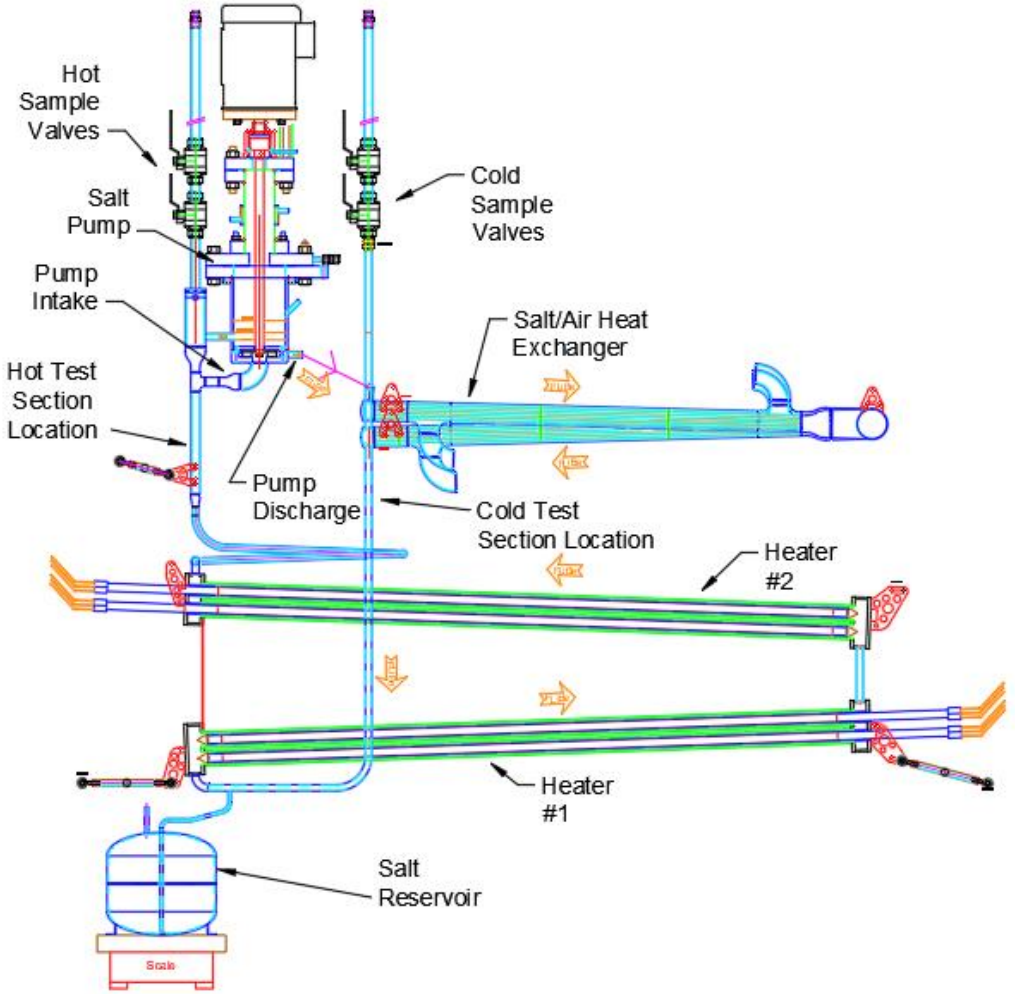

Figure 6: Schematic of the FCL's main components

Emissivity Measurement Methods

- Calorimetric
- Radiometric
  - **Direct emission**
  - Indirect reflectance

- Main advantage of radiometric methods is that spectral data provides additional information on surface state and can more accurately be used in non-gray scenarios

- Advantage of direct emission is much simpler optics and construction

- $\epsilon_{sample} = \epsilon_{reference} \frac{S_{sample}}{S_{reference}}$

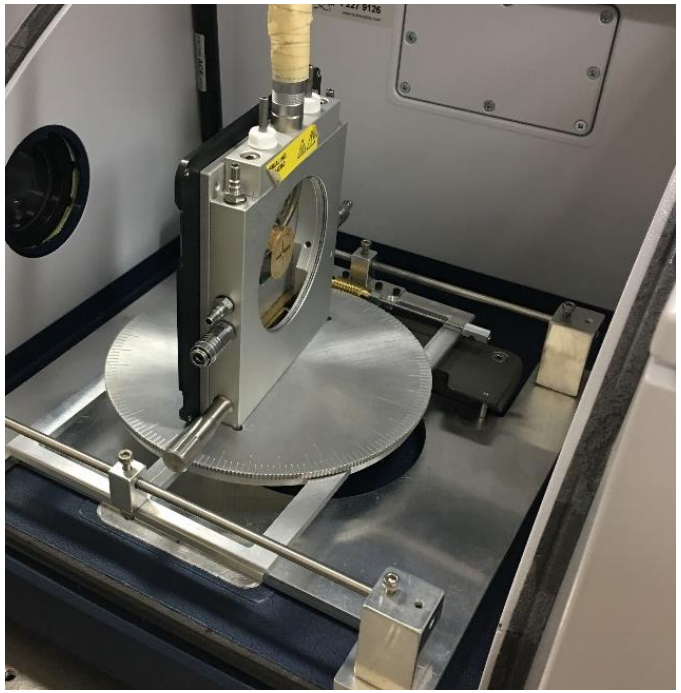

Heater Specs

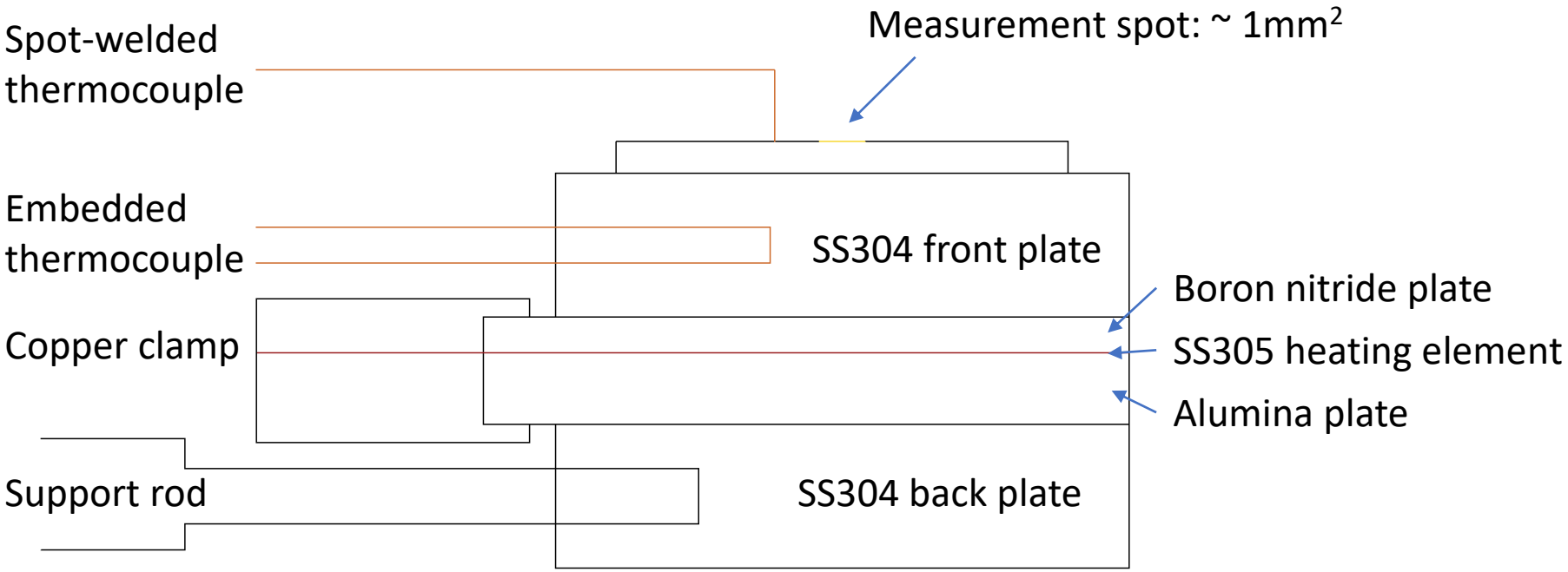

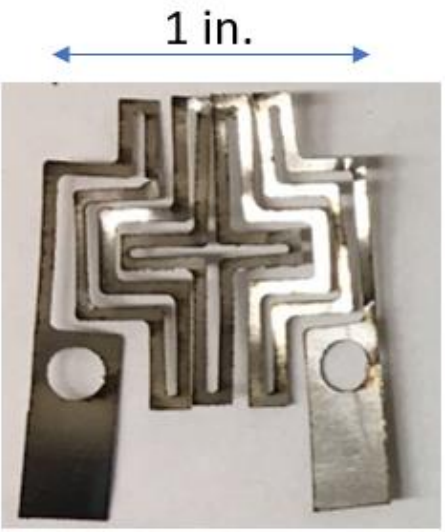

- SS304 front and back plates,
- SS305 sheet heating element
  - R = ~4.1 Ω (at room temp)
  - 0.002” thick
  - Max temp: ~1400 ˚C
- Boron nitride: high thermal conductivity electrical insulator
- Fired alumina (48% porosity): low thermal conductivity electrical insulator
- Embedded thermocouple: HH-K-24, potted with Ceramabond 671 ceramic paste
- Spot-welded thermocouple: 30 AWG bare wires

Material	Thickness [in.]	Max Temp[1] [˚C]	Thermal Conductivity [W/m*K]	Linear Thermal Expansion Coeff. [˚C^{-1}]	Density [kg/m^3]
SS304	0.25	~1400	16.2 (RT)	1.8E-5	7998
Boron Nitride	0.0625	~1800	46 (100 ˚C)	5.0E-7	2104
Alumina	0.125	~1700	0.64 (100 ˚C)	7.0E-6	2100

[1]Temperature limit of heater likely constrained by copper clamps (~1000 ˚C)

Top Flange Feedthroughs

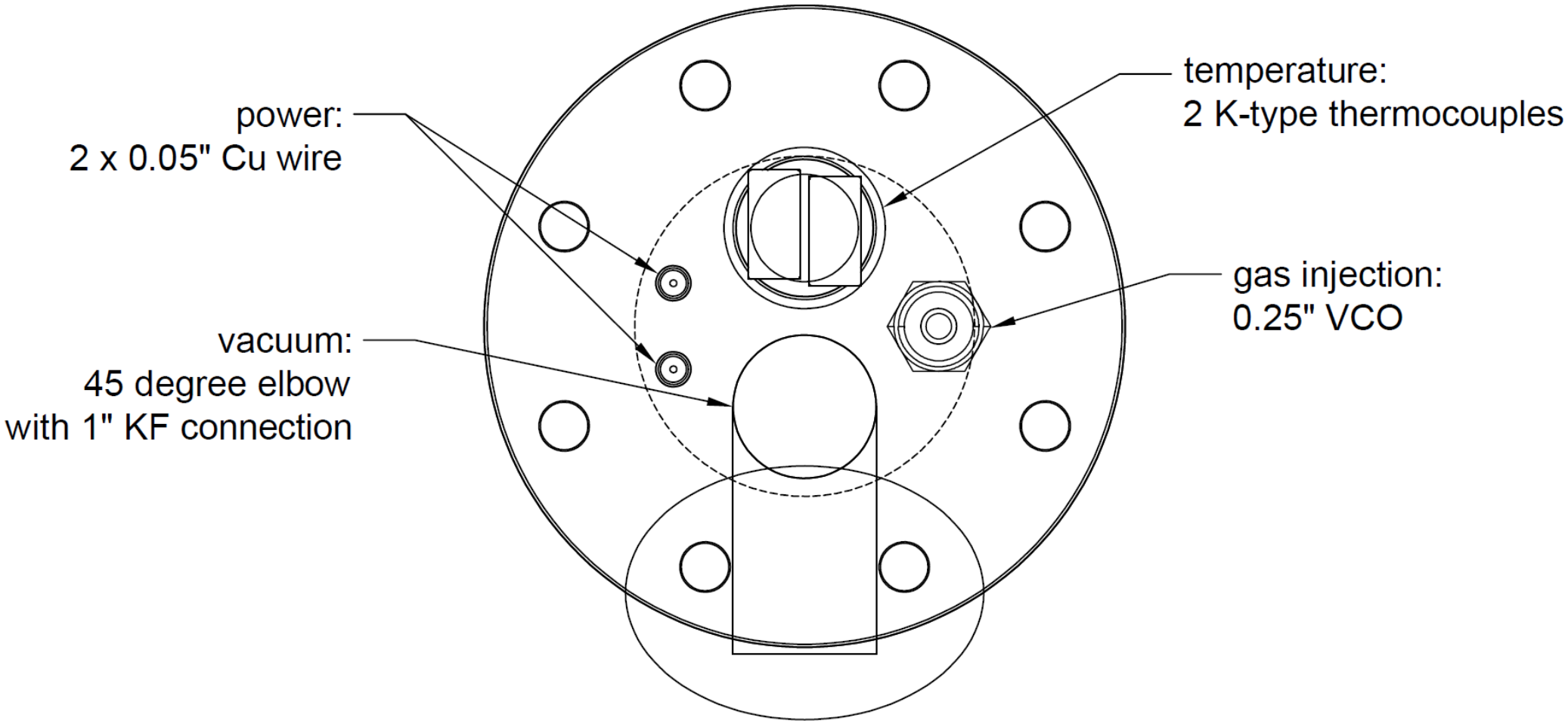

Emissivity Measurement Setup

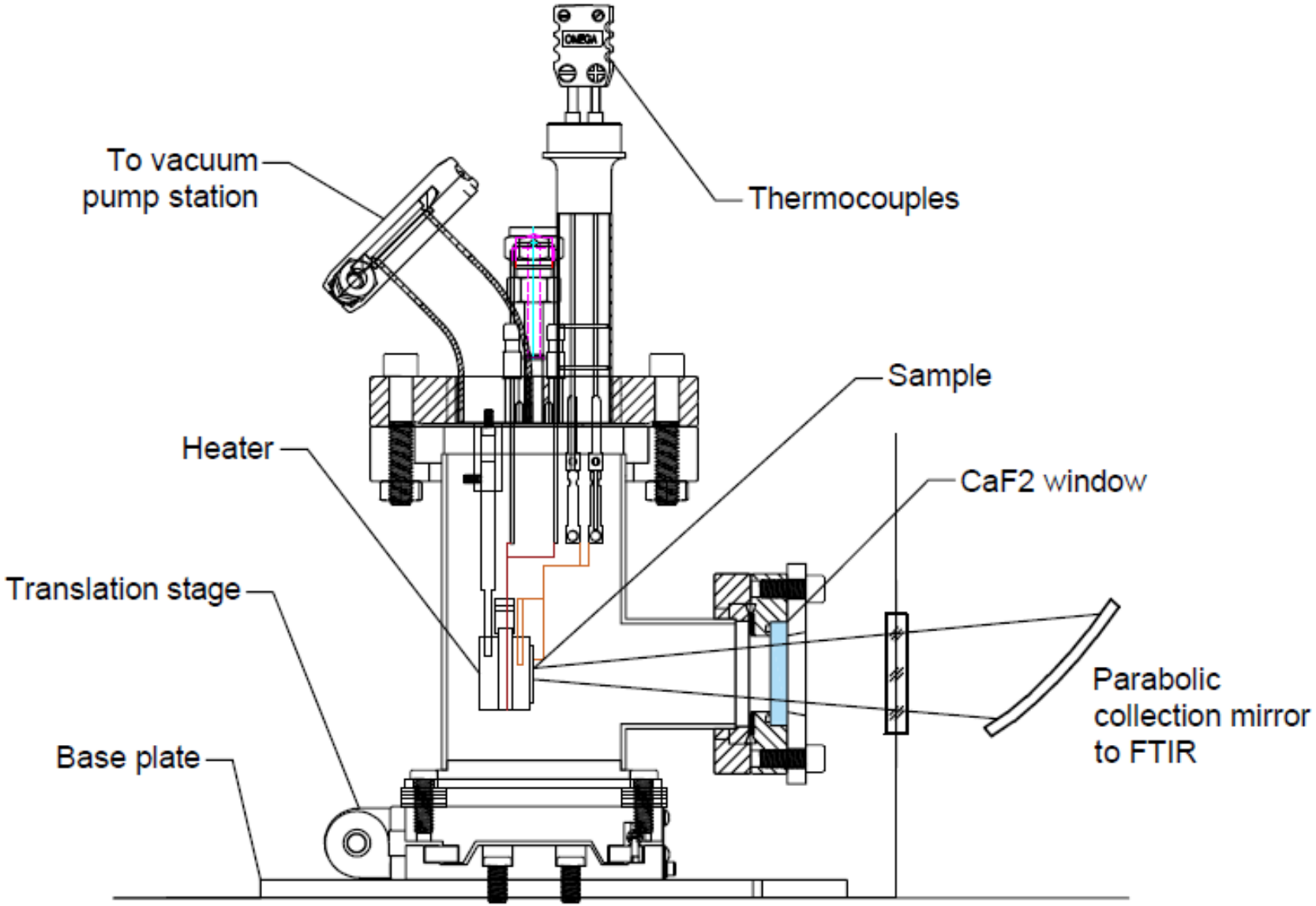

Measurement Capabilities

- Measurements performed at high vacuum (~1E-05 Torr) in order to prevent in-situ oxidation

- This limited the maximum temperature of the sample due to increased thermal resistance between the various layers
  - E.g. T_{stage} = 740 °C, T_{sample} = 600 °C
  - Decided to go with 520 °C for real samples

- Oxidation testing was performed with SA508 steel samples
  - Cr content of 0.15%
  - Sample held at 600 °C for 1.5 hours

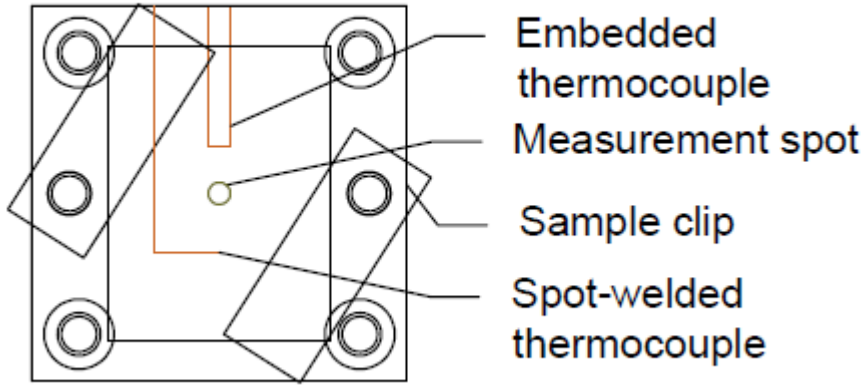

before

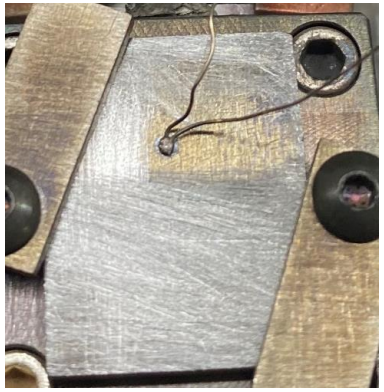

after

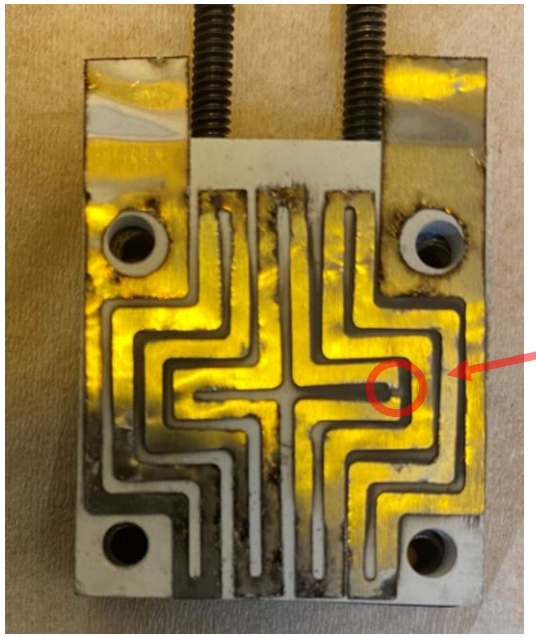

Optical Path

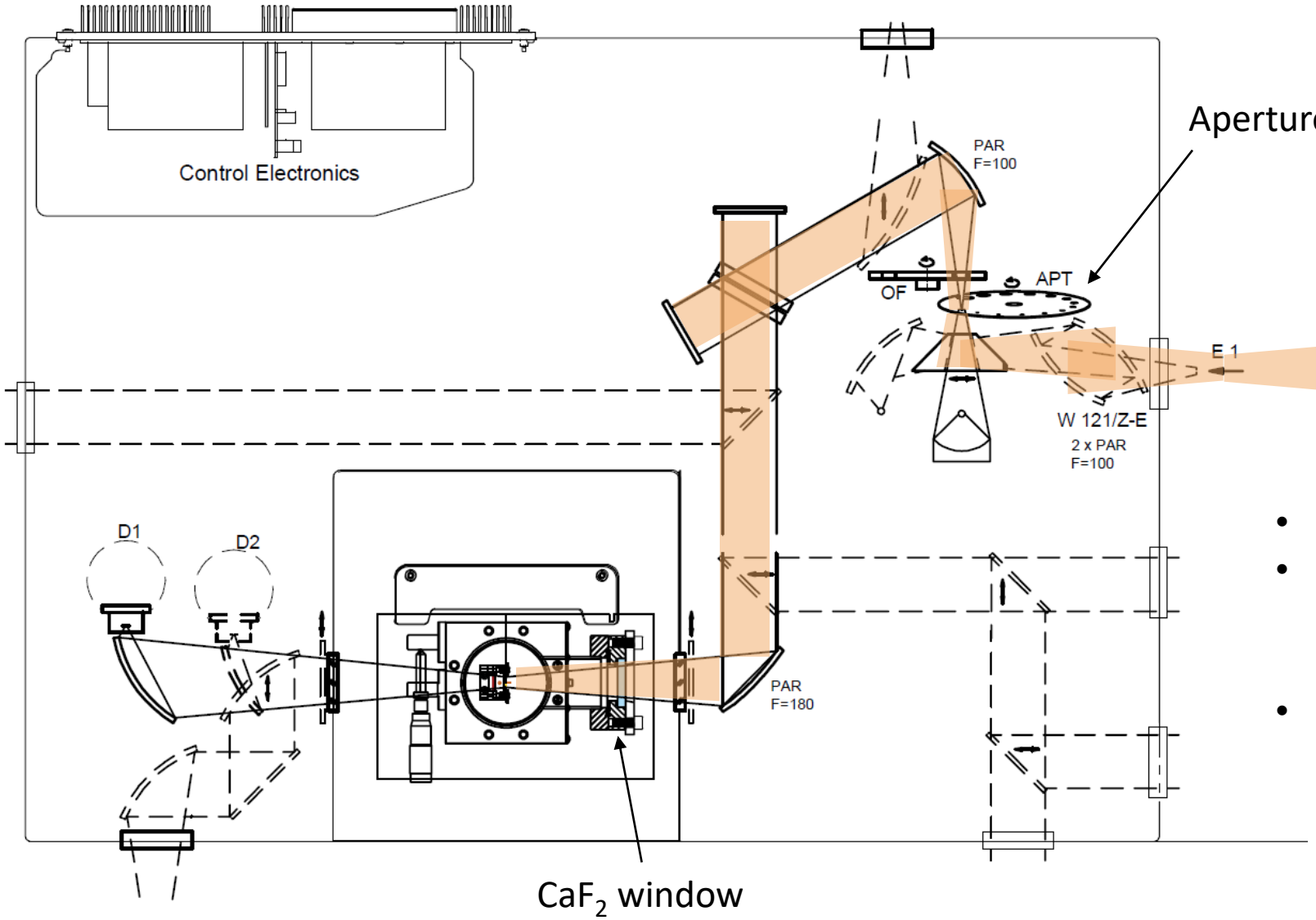

Aperture wheel

MCT Detector

- Optical diagram of Vertex 70 FTIR
- Not shown is Hyperion microscope, which has been simplified to be shown as the MCT detector
- N_2 purge of beam path to limit atmospheric absorption

Image of Setup

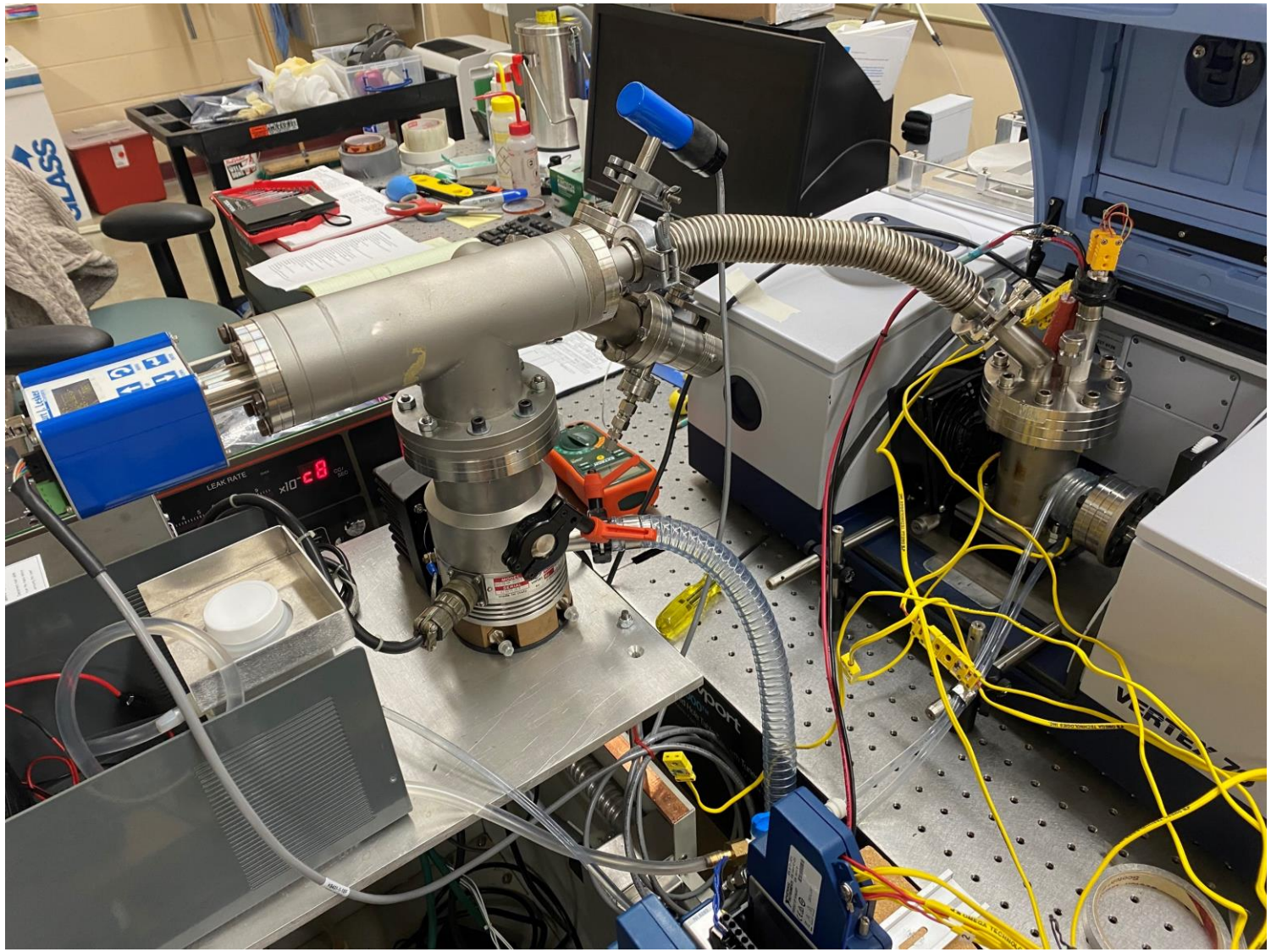

Blackbody Sample

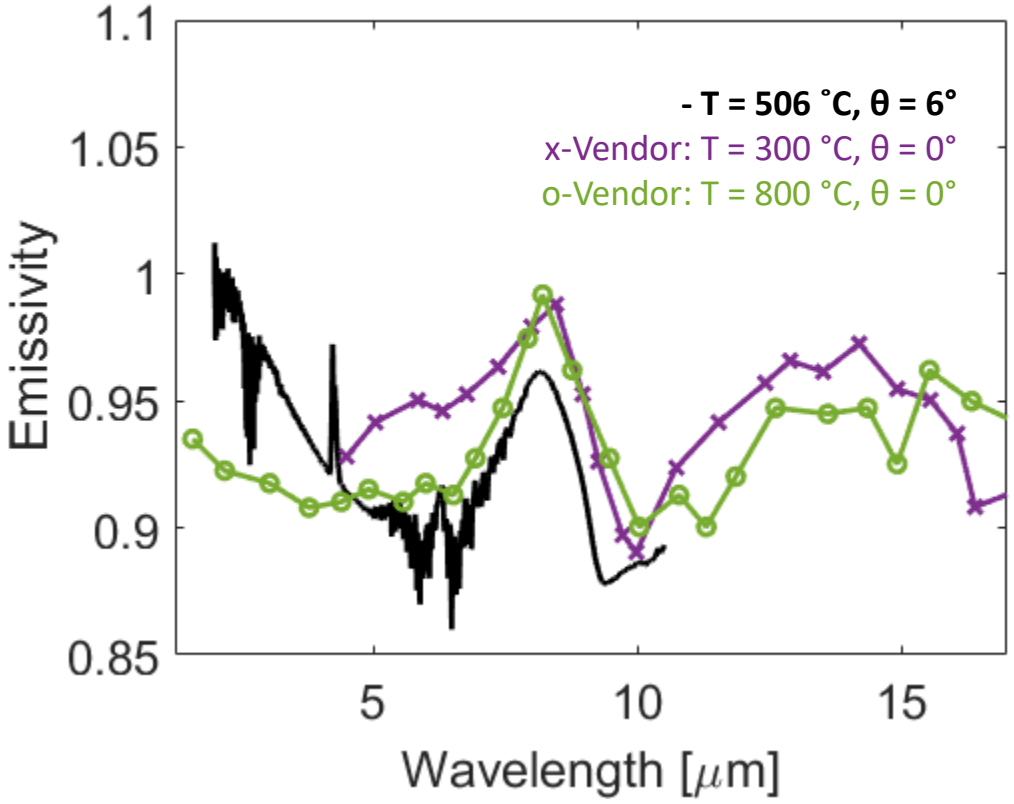

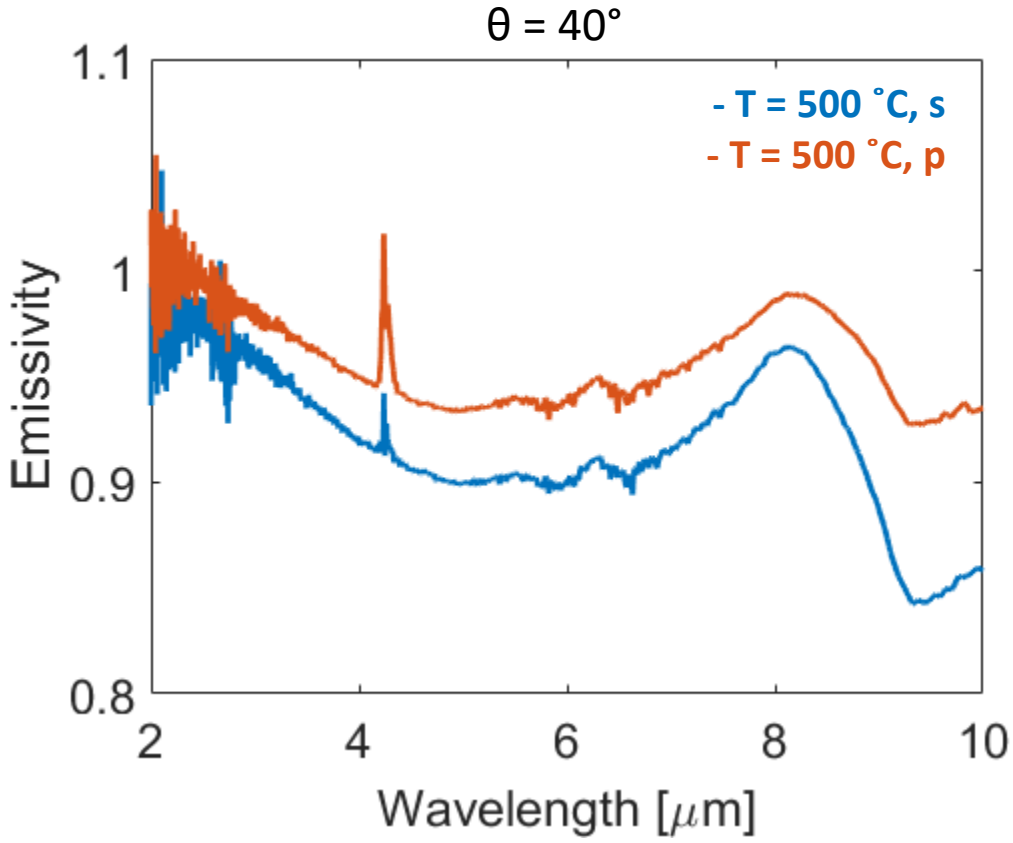

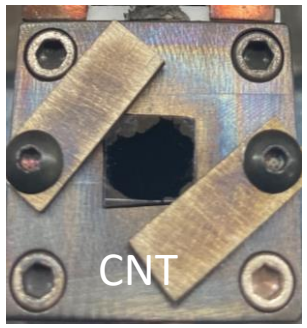

- Custom blackbody developed by applying Aremco™ 840M-HiE paint to sandblasted SS316 sample (same size as corrosion samples)
- referenced to CNT using calibration procedure
- $\epsilon_{paint} = \epsilon_{CNT} \frac{S_{paint}}{S_{CNT}} \frac{I_{bb}(T_{CNT})}{I_{bb}(T_{paint})}$

Validation Measurement

- Unexposed SS316 sample measurent compared against indirect method (integrating sphere).
- The slight increase is consistent with Hagen-Rubens theory, which predicts the 500 ˚C emissivity should be higher by about 0.05
- Wide-angle emissivity starts to increase at about 7 µm. This behavior is not expected and is likely due to background emission by enclosure walls
- $\epsilon_{SS316} = \epsilon_{paint} \frac{S_{SS316}}{S_{paint}} \frac{I_{bb}(T_{paint})}{I_{bb}(T_{SS316})}$

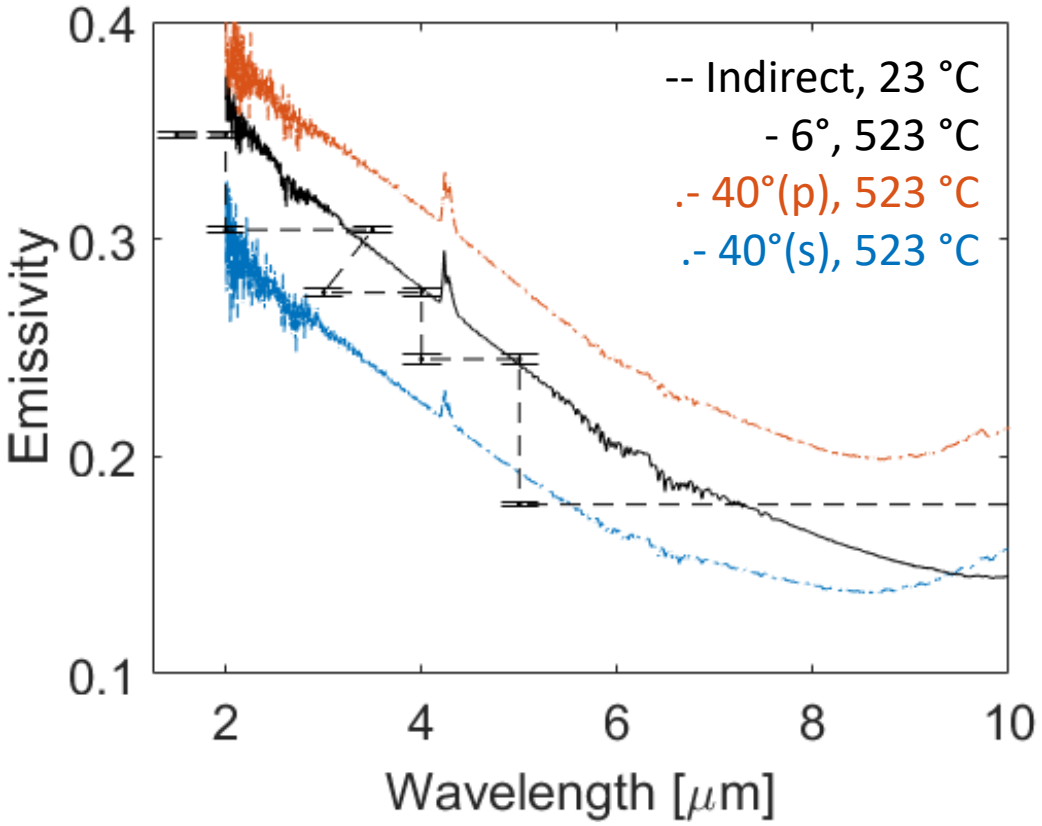

Exposed Sample Results

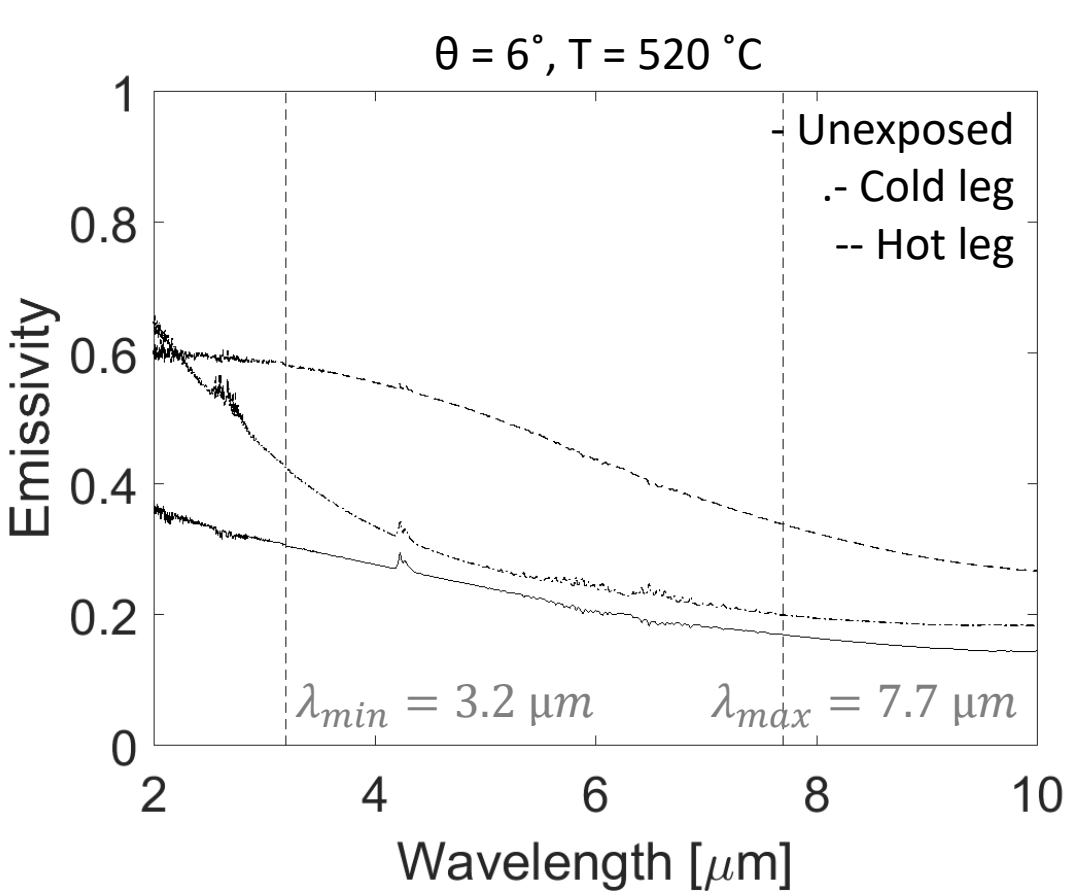

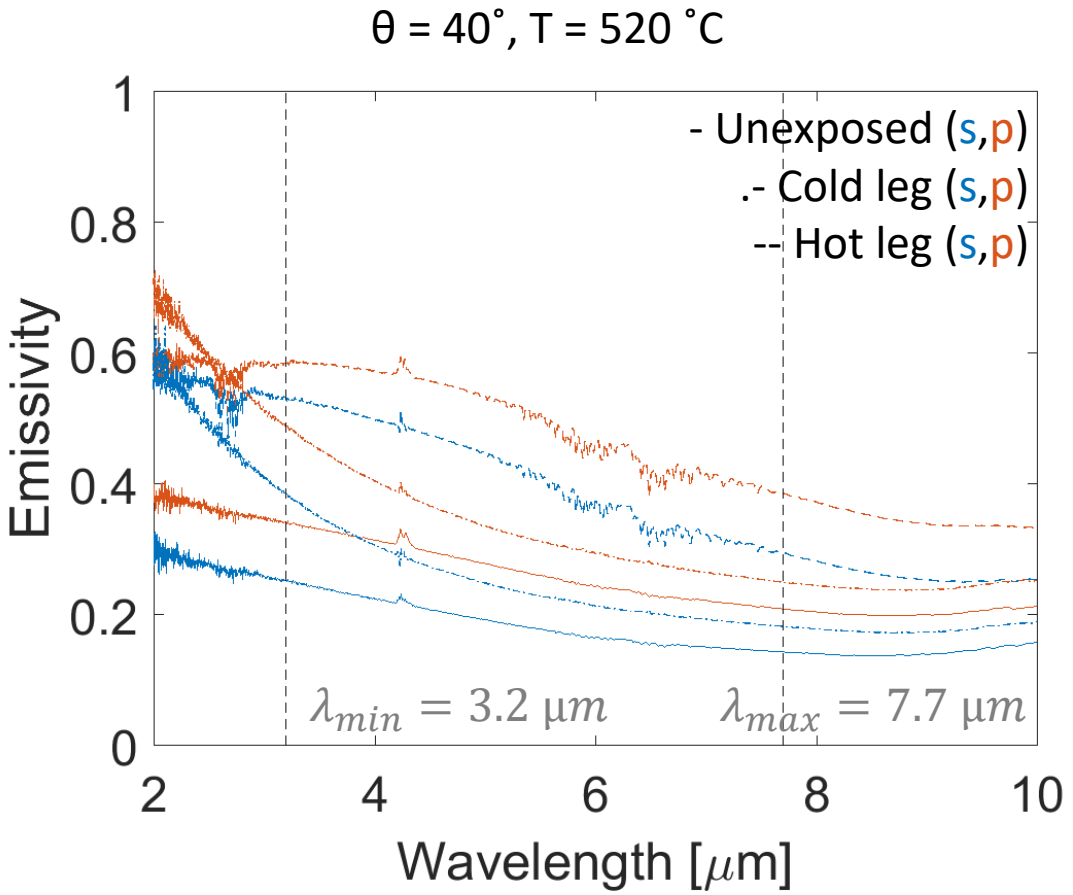

- Cold leg sample emissivity increased during dry run and the results are considered an upper bound of the emissivity of the sample post-exposure
- Hot leg sample emissivity is larger than both unexposed and cold leg (except from 2-3 μm)
- 40° data consistent with 6°

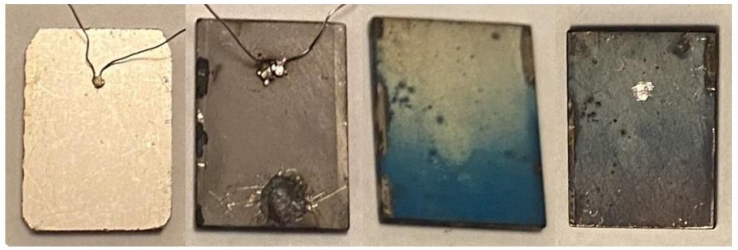

Unexposed | Hot leg | Cold leg (after dry run) | Cold leg (before dry run)

Error Model

$$S_\alpha = m[\epsilon_\alpha I_{bb}(T_\alpha) + \epsilon_{enc}(1-\epsilon_\alpha) I_{bb}(T_{enc}) + B_{ins}]$$

$$\epsilon_{ss} = \epsilon_p \frac{S_{ss}}{S_p} \frac{I_{bb}(T_p)}{I_{bb}(T_{ss})}$$

$$\left[\frac{S_{ss}}{S_p}\frac{I_{bb}(T_p)}{I_{bb}(T_{ss})}\right]_{meas} = \left[\frac{\epsilon_{ss}}{\epsilon_p}\right]_{true} \cdot \Delta_{ss} \cdot \sigma_Q \cdot \sigma_{cold} \cdot var + \sigma_{enc} + \sigma_{ins}$$

- $\sigma_{\epsilon_p} = \pm 0.05$, determined via calibration and heterogeneity testing
- $\Delta_{ss} = \frac{\epsilon_{ss,before}}{\epsilon_{ss,after}} = 1 + \sigma_{\Delta_{ss}}$; determined via before/after testing
- $\sigma_Q = \frac{I_{bb}(T_{ave}+\Delta_{TC})}{I_{bb}(T_{ave})} = 1 \pm (1 - \frac{I_{bb}(T_{ave}+\Delta_{TC})}{I_{bb}(T_{ave})})$; $\Delta_{TC} = \sigma_{T_{ss}} - \sigma_{T_p}$; $T_{ss,meas} = T_{ss,true} + \sigma_{T_{ss}}$, $T_{p,meas} = T_{p,true} + \sigma_{T_p}$
- $var = 1 \pm \sigma_{var}$; determined via heterogeneity testing
- $\sigma_{cold} = \frac{I_{bb}(T_{ss,stage})}{I_{bb}(T_{ss,spot})} = 1 - (1 - \frac{I_{bb}(T_{ss,stage})}{I_{bb}(T_{ss,spot})})$, for cold leg sample only
- $\sigma_{enc} = -(1-\epsilon_\alpha)\frac{I_{bb}(T_{enc})}{I_{bb}(T_{ave})}$; assume $\epsilon_\alpha = 0$ as bounding case
- $\sigma_{ins} = +\epsilon_{ss,m2} - \epsilon_{ss,m1}$

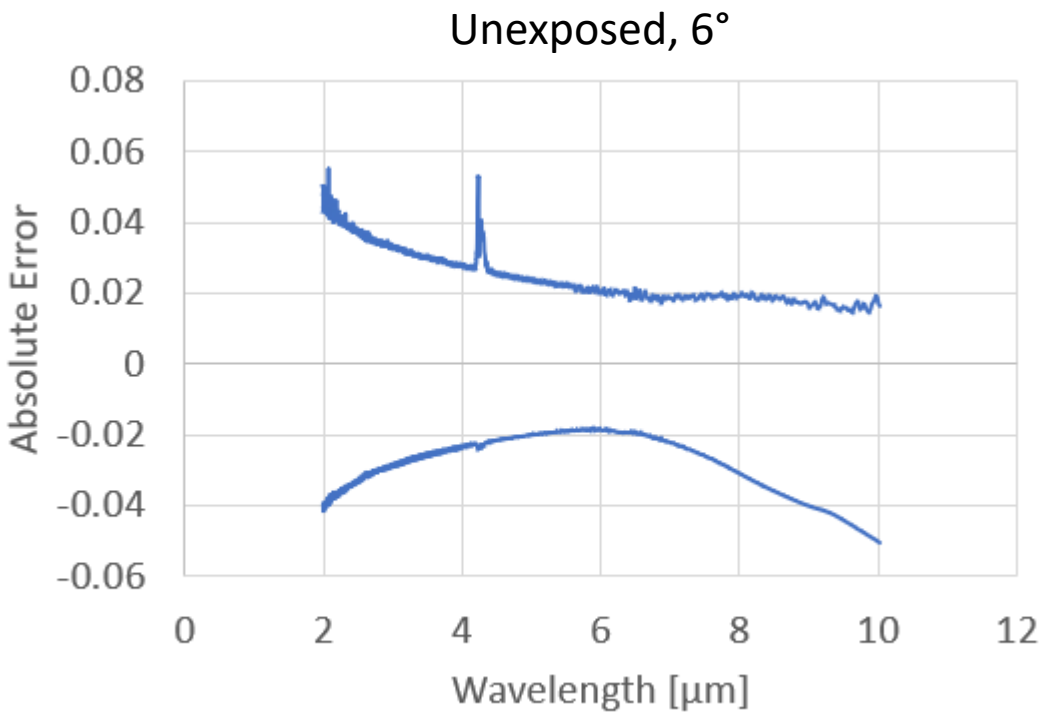

Comparison with Literature

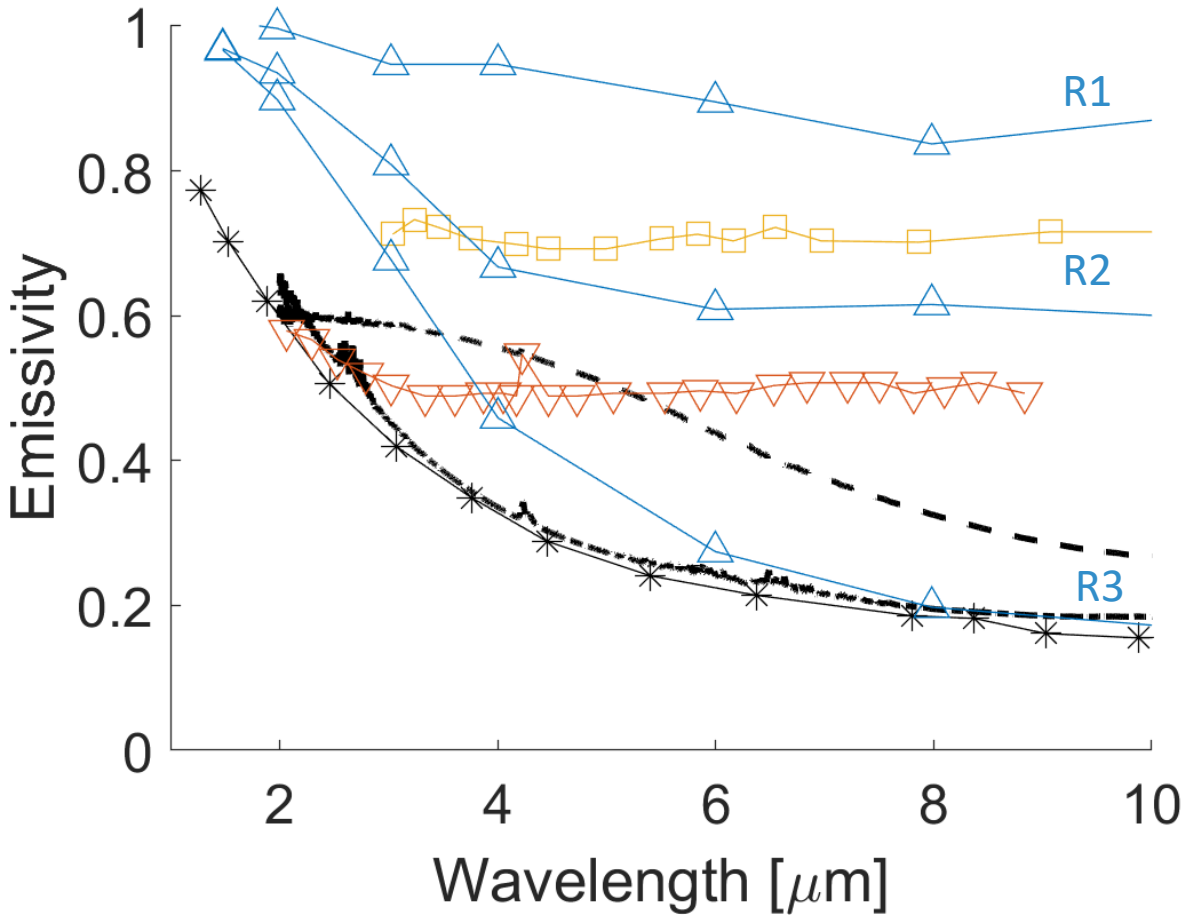

-Δ 304, Rolling (R1): wet H_2, 1000 °C for 90 min (1.40 µm) [2]
-Δ 304, Rolling (R2): wet H_2, 1000 °C for 30 min (0.95 µm) [2]
-Δ 304, Rolling (R3): wet H_2, 800 °C for 30 min (0.17 µm) [2]
-□ 316, King: flowing sCO_2, 650 °C for 400 hours [1]
-∇ 316, Cao: air, 700 °C for 5 hours [3]
-* 316, King: static FLiBe, 700 °C for 1000 hours [1]
-- Hot leg
.- Cold leg

[1] J. L. King, H. Jo, et al., 'Impact of Corrosion on the Emissivity of Advanced Reactor Structural Alloys', *J. Nucl. Mater.*, **vol. 508**, pp. 465–471, (2018).
[2] R. E. Rolling and A. I. Funai, 'Investigation of the Effect of Surface Conditions on the Radiant Properties of Metals, Technical report No. AFML-TR-64-363, Part II', *Lockheed Missiles Sp. Co.*, (1967).
[3] G. Cao, S. J. Weber, et al., 'Spectral emissivity of candidate alloys for very high temperature reactors in high temperature air environment', *J. Nucl. Mater.*, **vol. 441**, no. 1–3, pp. 667–673, (2013).

- Cold leg sample shows signs of oxide film, but at least some of this formed during the dry run. Agreement with King's data indicates that his sample probably had a similar level of oxidation. Both are close to Rolling 3S, indicating an oxide layer of slightly less than 0.17 µm
- Hot leg could be due to oxidation, but doesn't line up exactly with any curves from literature

Surface SEM and EDS mapping of F

Hot leg

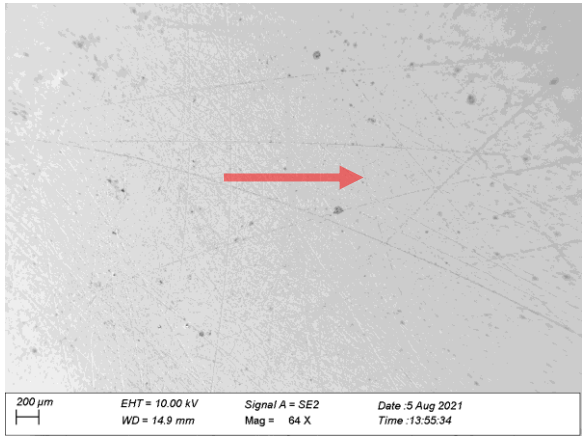

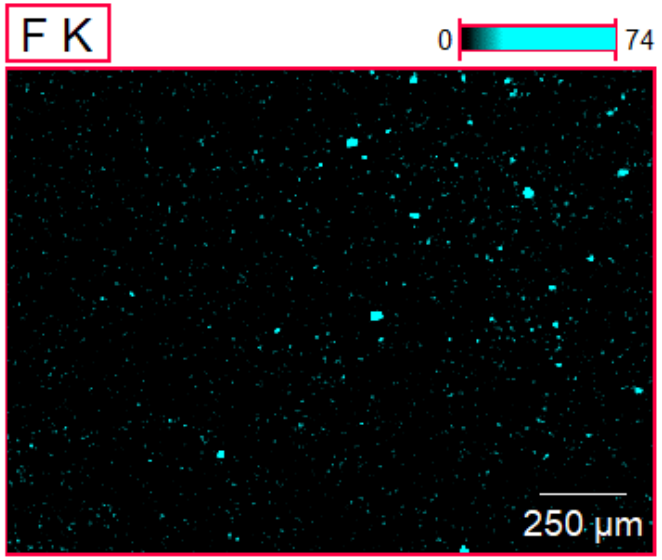

Cold leg

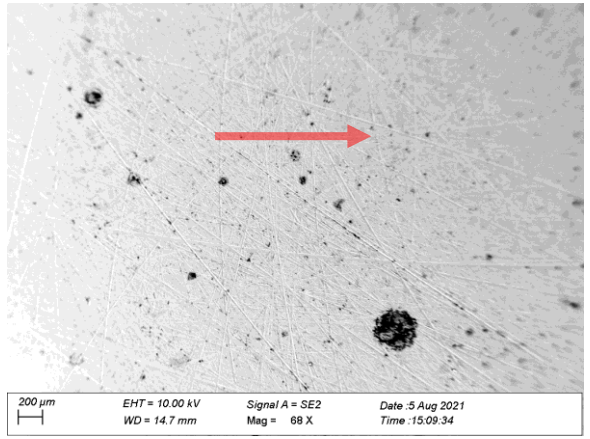

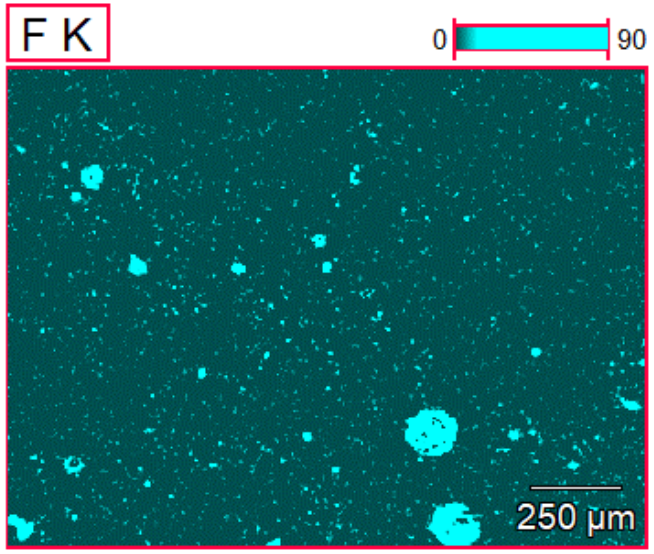

More salt present on cold leg, could have been source of moisture release during dry run

Surface EDS Linescans

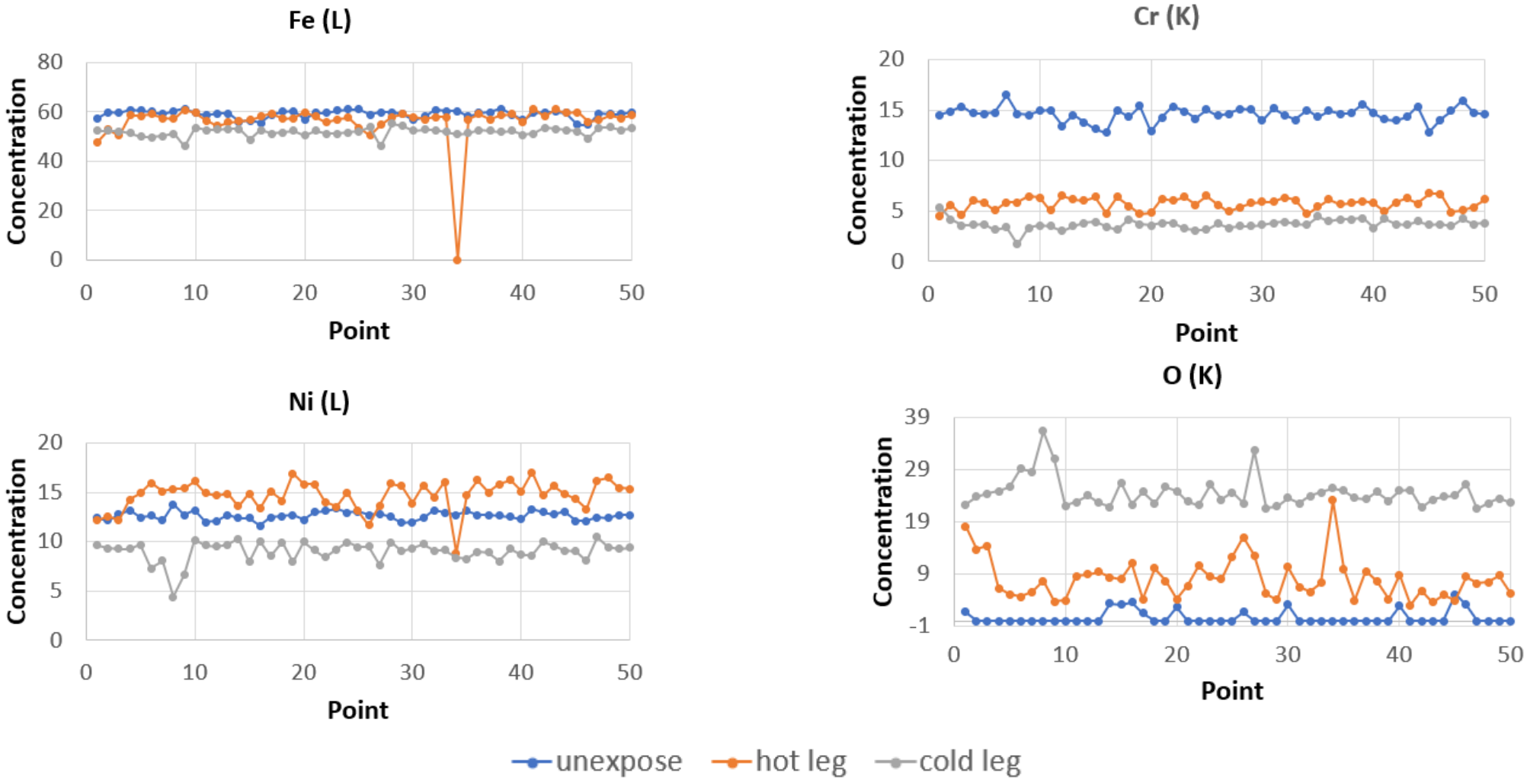

- Similar Cr depletion between cold leg and hot leg
- Large O concentration on cold leg could explain insulating effect which prevented spot welding

Roughness Measurements

Hot leg

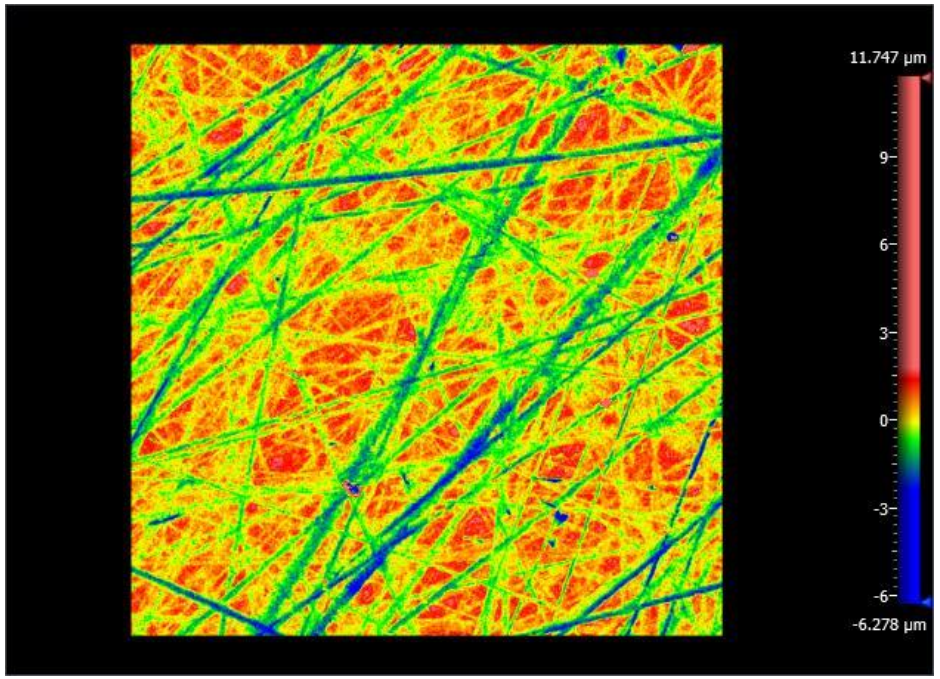

Cold leg

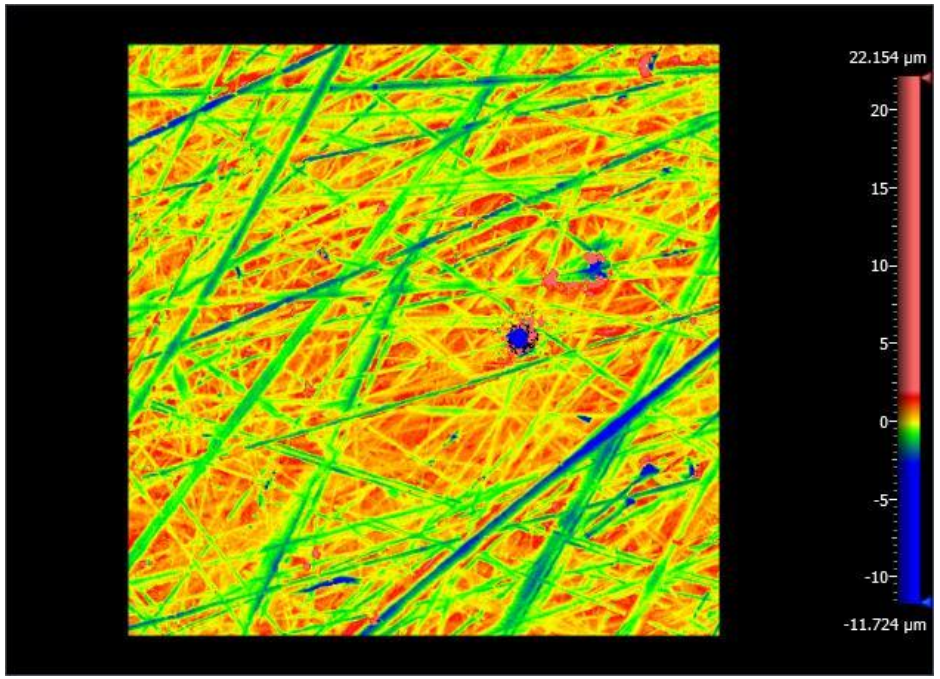

	Cold Leg	Hot Leg
RMS [µm]	0.77±0.10	0.78±0.02
PV [µm]	5.6±2.7	5.2±0.2

Surface roughness too similar to explain emissivity differences

Hot Leg: Cross Sectional EDS Linescans

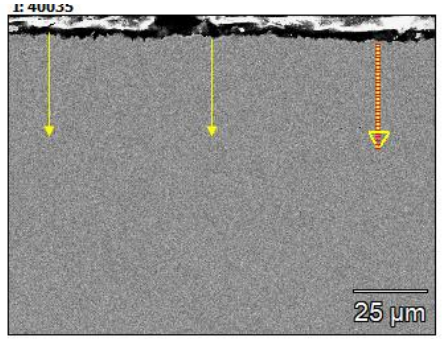

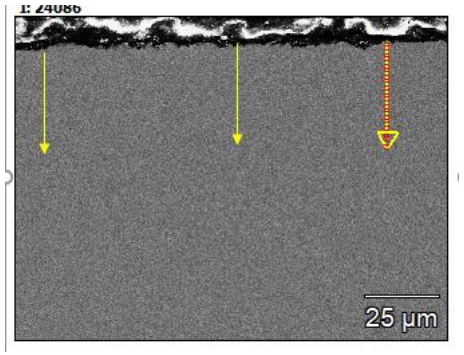

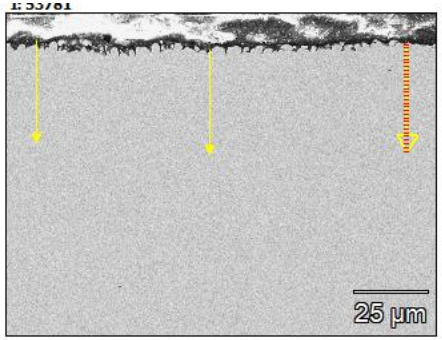

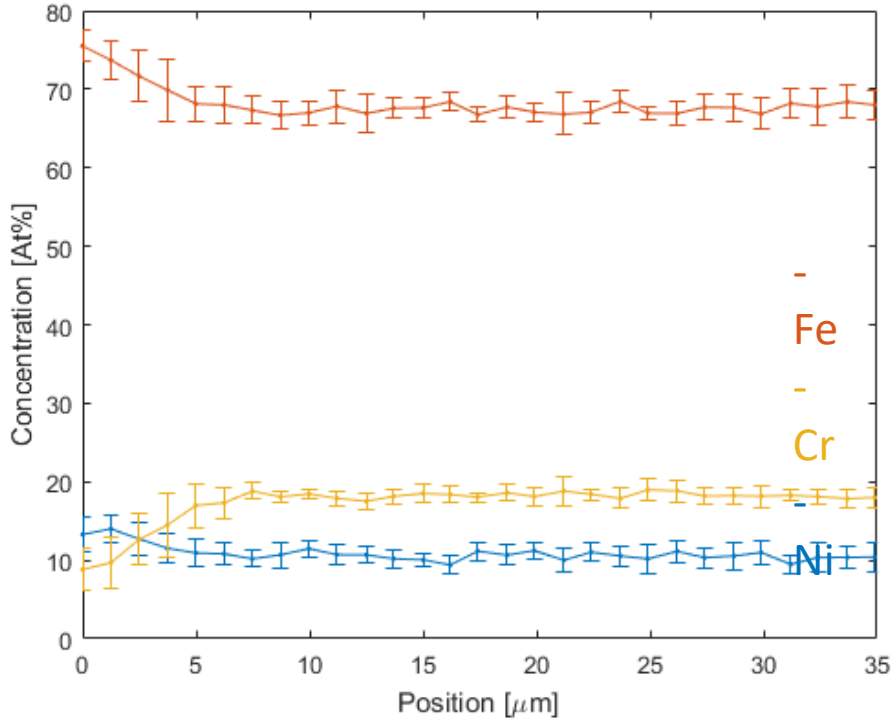

- Averaged over 9 line scans performed at 3 separate spots
- Cr depletion is expected and would explain formation of oxide film (after salt exposure)
- Slight Fe and Ni enrichment

Hot Leg: Cross Sectional SEM Image

- Small film or deposited layer of some kind appears present at corrosion interface
- Precipitates may have formed in bulk

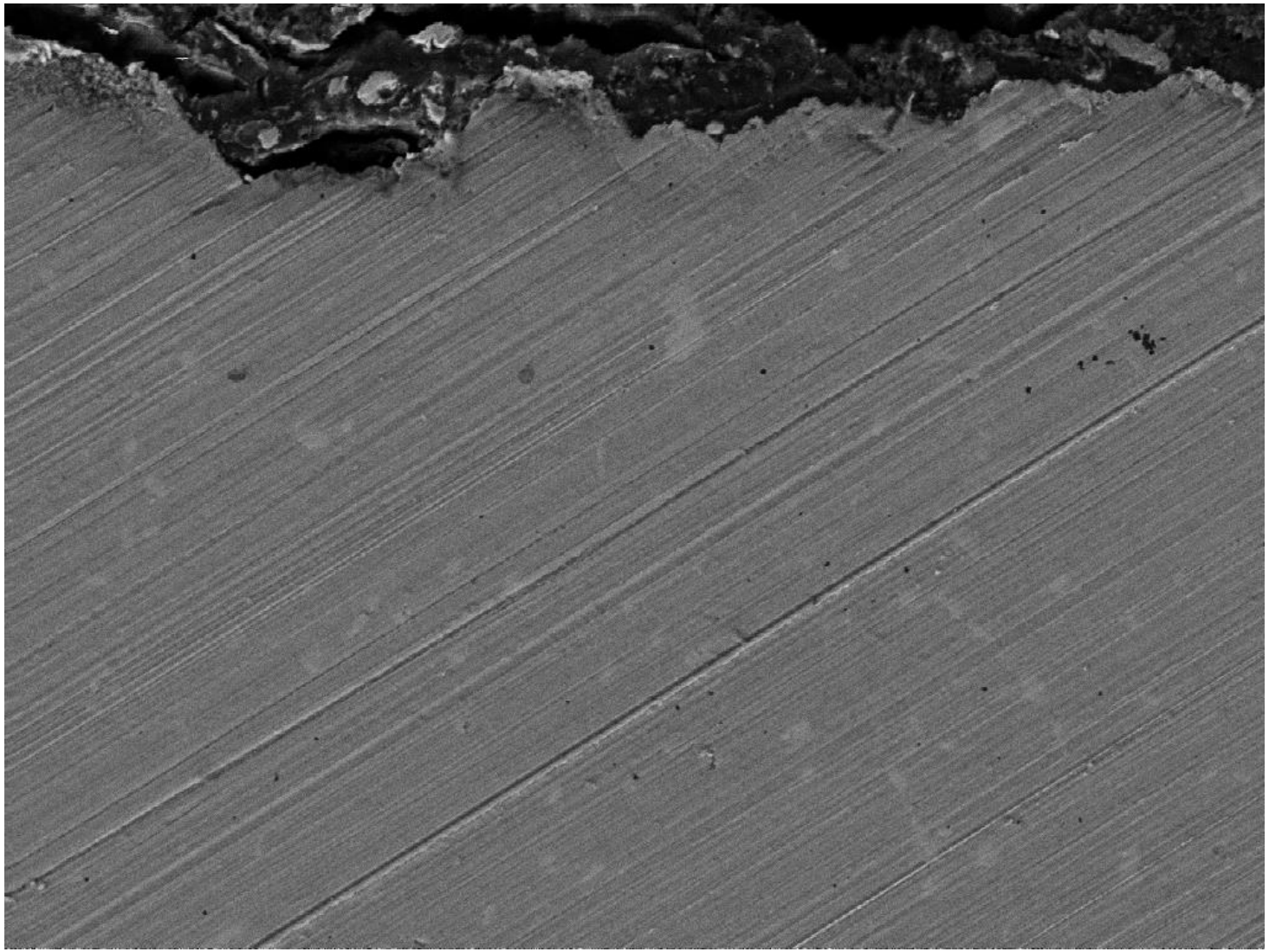

Conclusions.. TBD

- Cold leg sample to be imaged to check corrosion profile and for signs of oxide film

- Cold leg data provides good upper bound of in-salt SS316 emissivity for cold surfaces
- Hot leg exposure is correlated with a greater emissivity increase relative to cold leg exposure. Analysis is pending as to whether this is correlated with increased corrosion
- It is most likely that a thin oxide film formed on the cold leg sample after salt exposure, evidenced by the blue color. This could have occurred after the salt drained and the samples cooled to ambient temperature. This film grew during the dry run due to moisture released by residual salt
- The exact mechanism for the emissivity increase in the hot leg is not known. It could be due to enhanced oxidation caused by the higher exposure temperature; however, the surface EDS line scans cast some doubt

Online Monitoring of Fission Products in 3LiCl-2CsCl

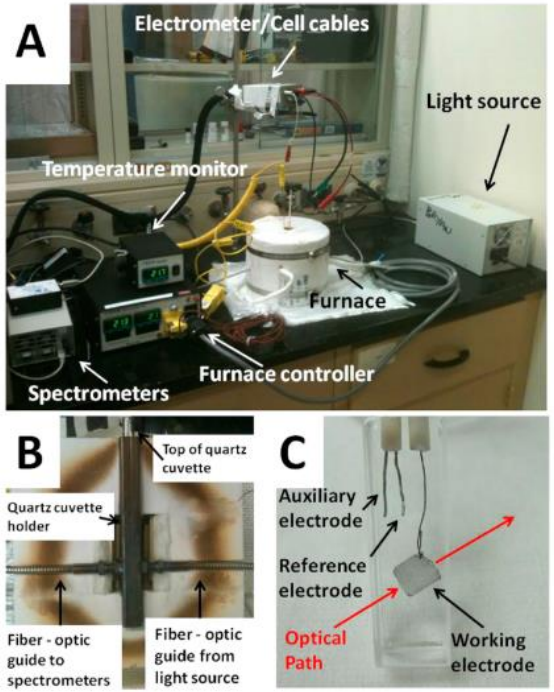

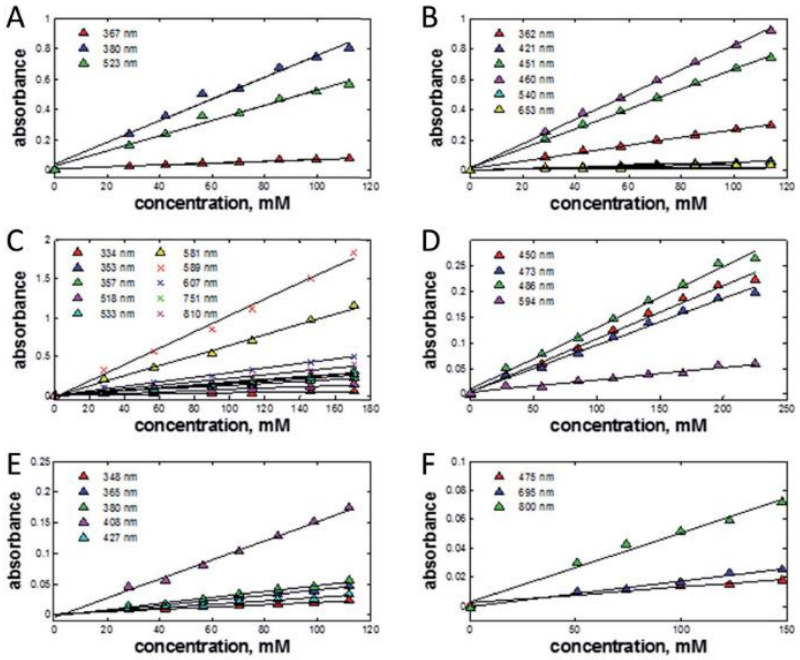

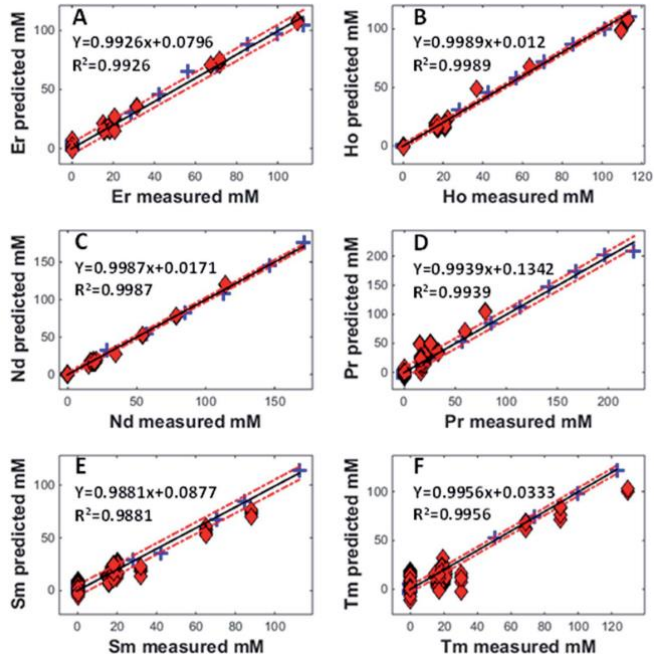

Electrochemistry and Spectroelectrochemistry of Europium(III) Chloride in 3LiCl–2KCl from 643 to 1123 K

Cynthia A. Schroll,[†] Sayandev Chatterjee,[‡] Tatiana G. Levitskaia,[‡] William R. Heineman,*[,†] and Samuel A. Bryan*[,‡]

Absorption spectroscopy for the quantitative prediction of lanthanide concentrations in the 3LiCl–2CsCl eutectic at 723 K†

Cynthia A. Schroll,[a] Amanda M. Lines,[b] William R. Heineman*[a] and Samuel A. Bryan*[b]

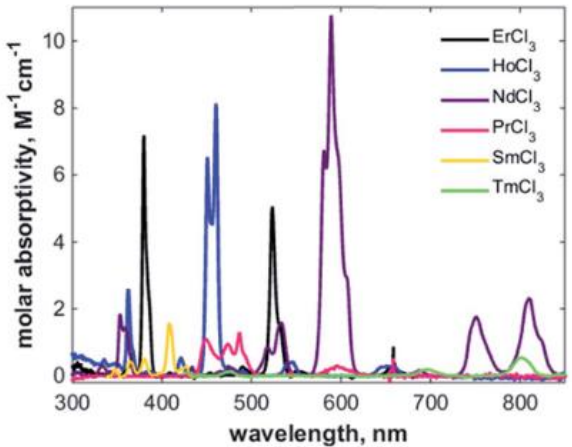

- High temperature fiber optic cuvette inside of ceramic furnace
- Calibration of various fission products via single-component measurements
- Prediction of fission product concentrations in multi-component samples

Vis/NIR Absorption of Corrosion Products in FLiBe

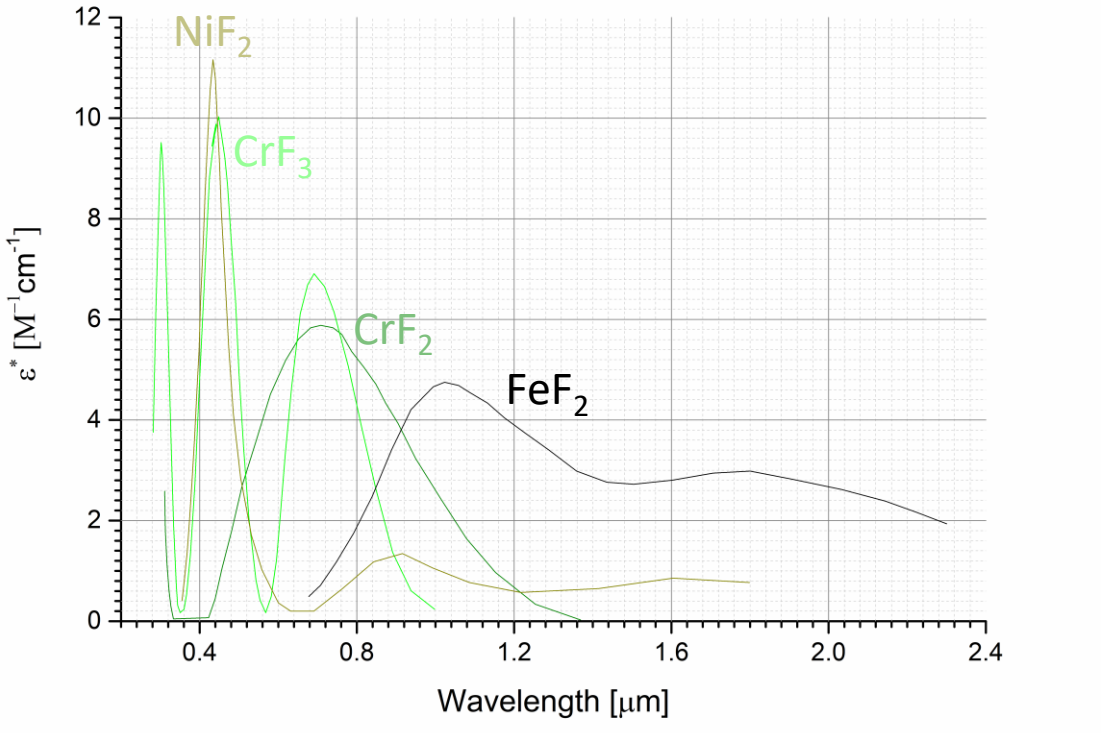

Absorption Spectra of Several 3d Transition Metal Ions in Molten Fluoride Solution[1,2]

By J. P. YOUNG

Received August 20, 1968

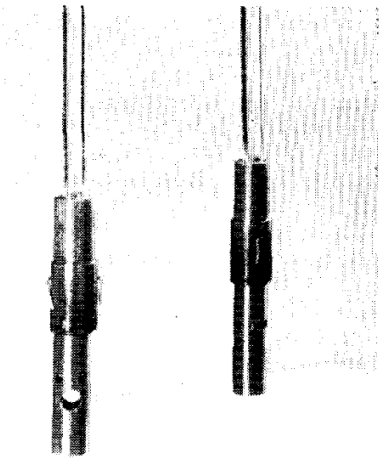

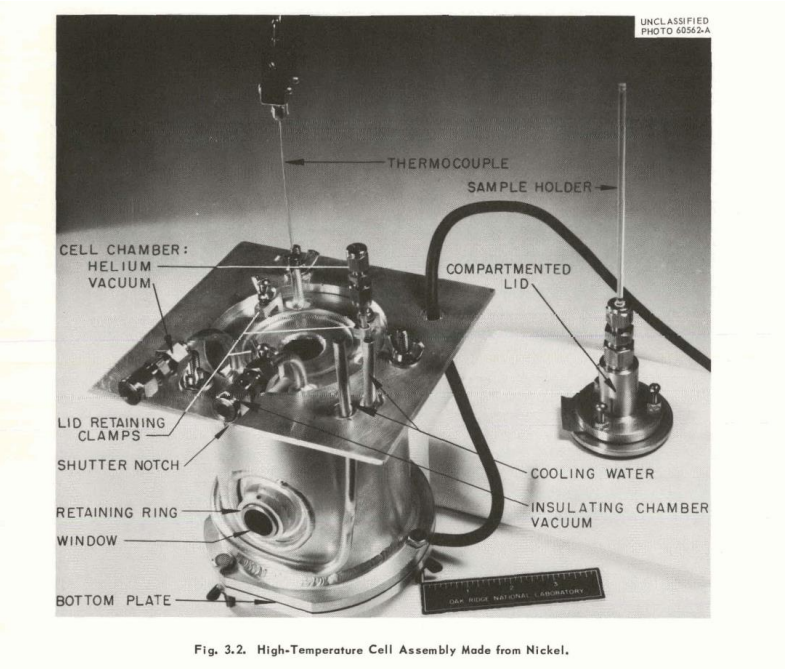

Fig. 3.2. High-Temperature Cell Assembly Made from Nickel.

- FeF_2, NiF_2, CrF_2, and CrF_3 in FLiBe were measured at 540-550 ˚C by Young using graphite windowless cell and sealed, water-cooled furnace assembly
- Inside of tube: inverted Ni Tee sitting inside metal block and surrounded by heater rods
- Furnace assembly fit into spectrometer sample compartment

Graphite Cell with Diamond Windows

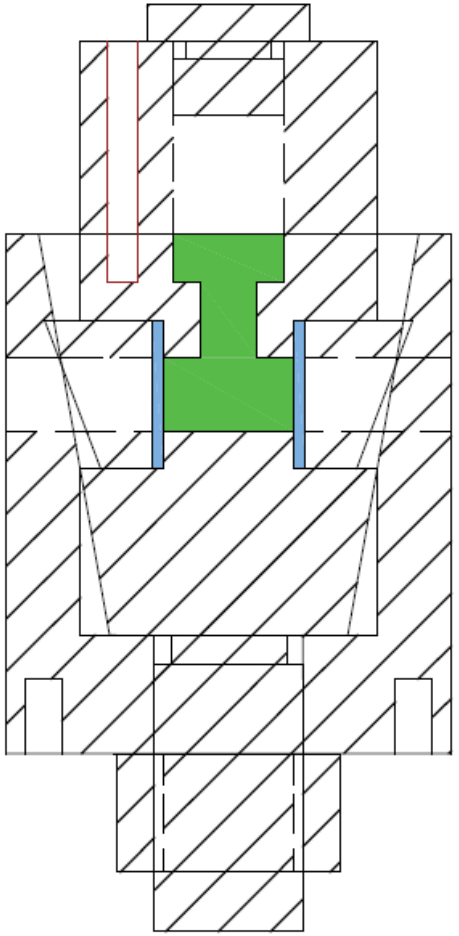

Window clamped inside of lip, but no o-ring seal. Salt is contained via surface tension because it does not wet graphite

Optical Absorption Setup

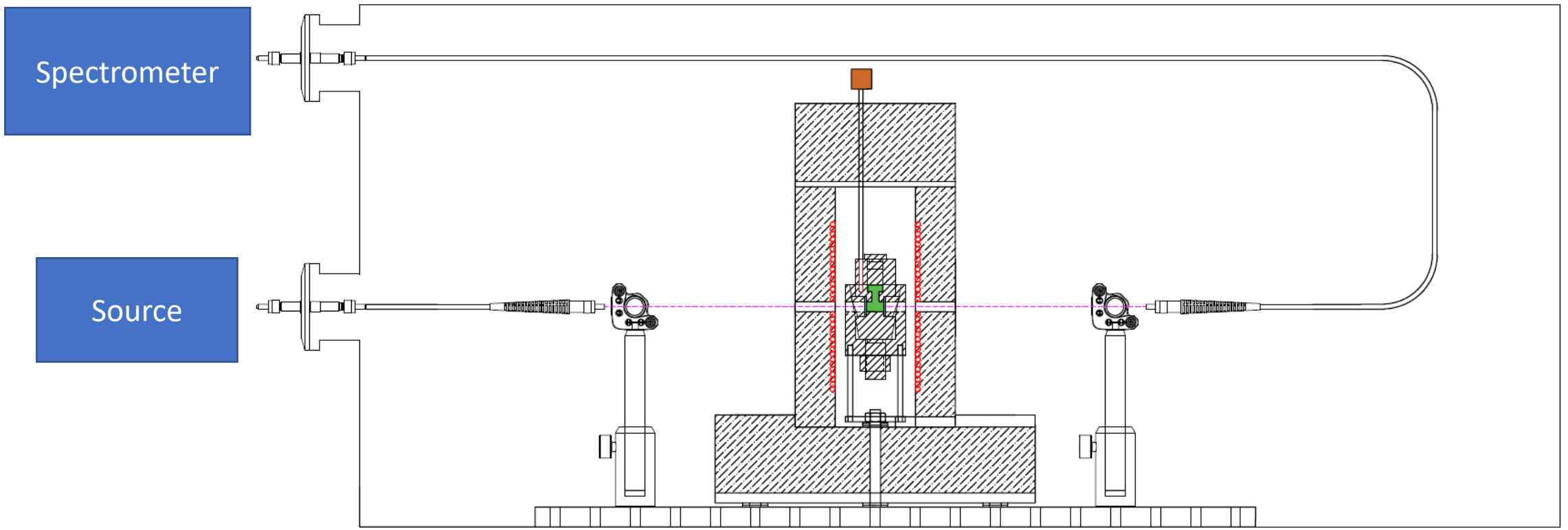

Setting up outside of Glovebox

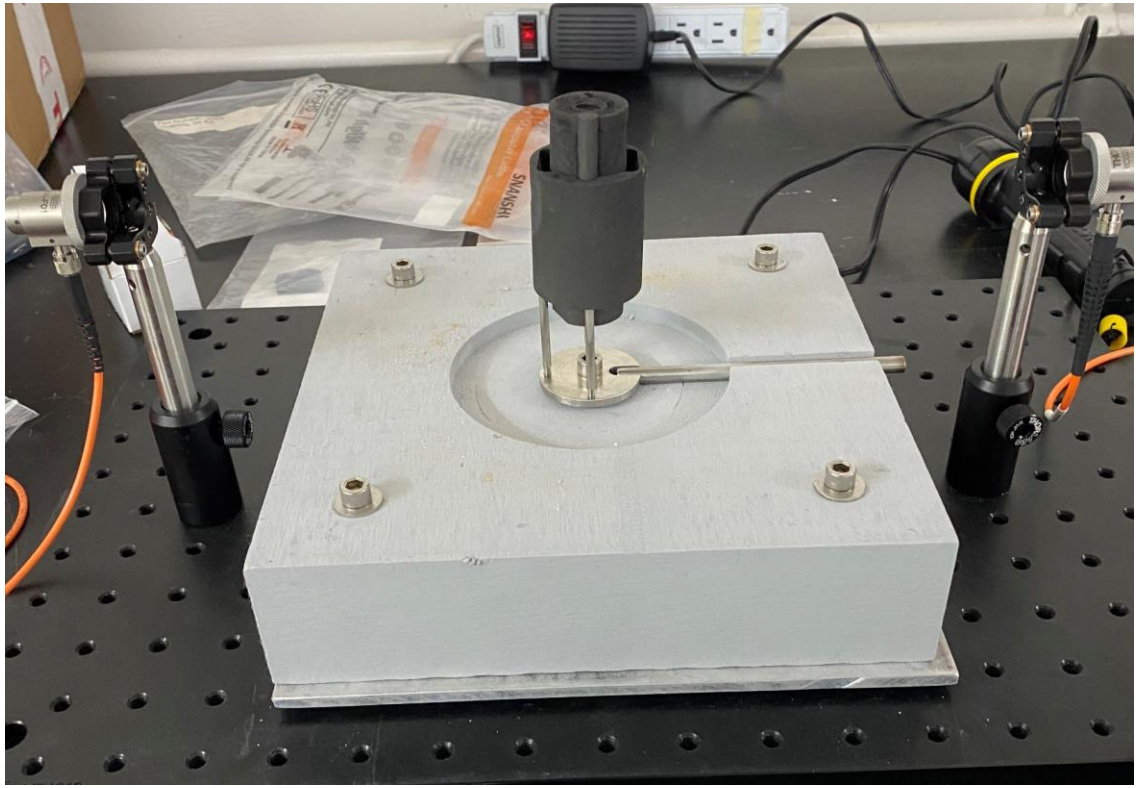

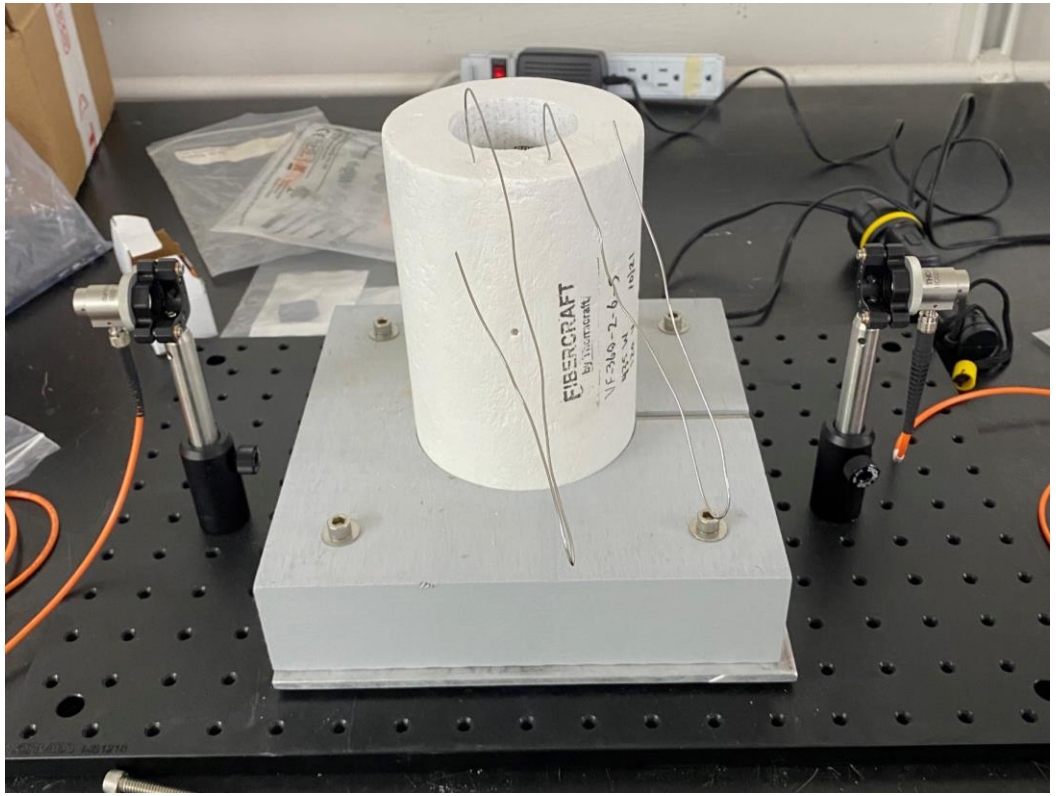

Calibration measurements

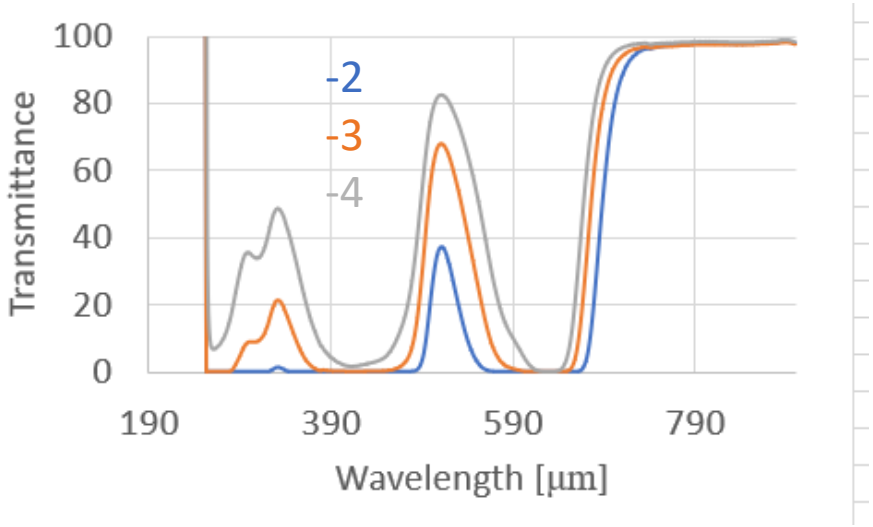

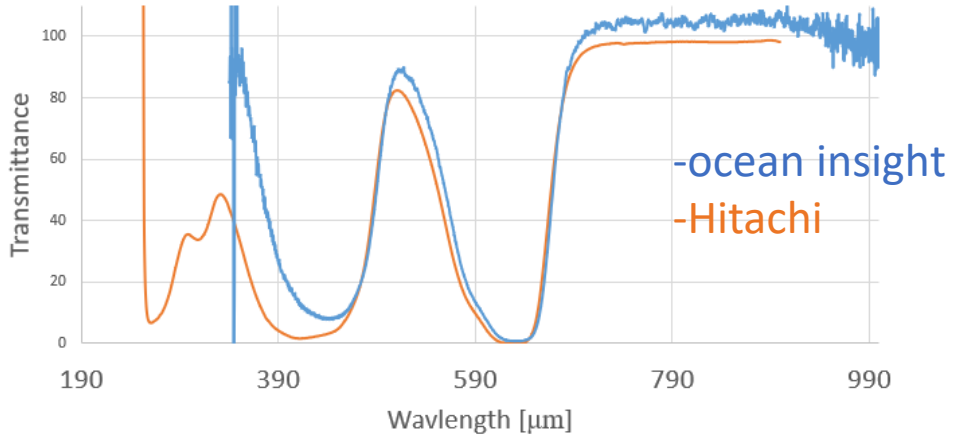

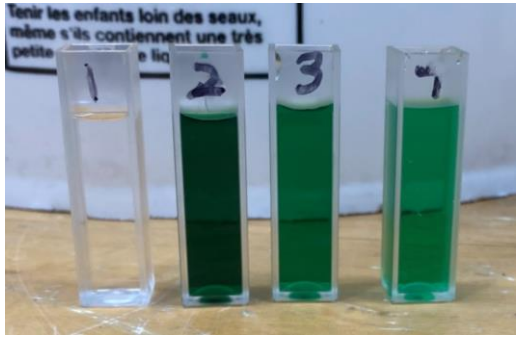

- Rough calibration measurements with DI water and diluted green dye performed using Hitachi UV-Vis spectrometer
- Measuring solution #4 using molten salt absorption setup

Nitrate Salt measurements

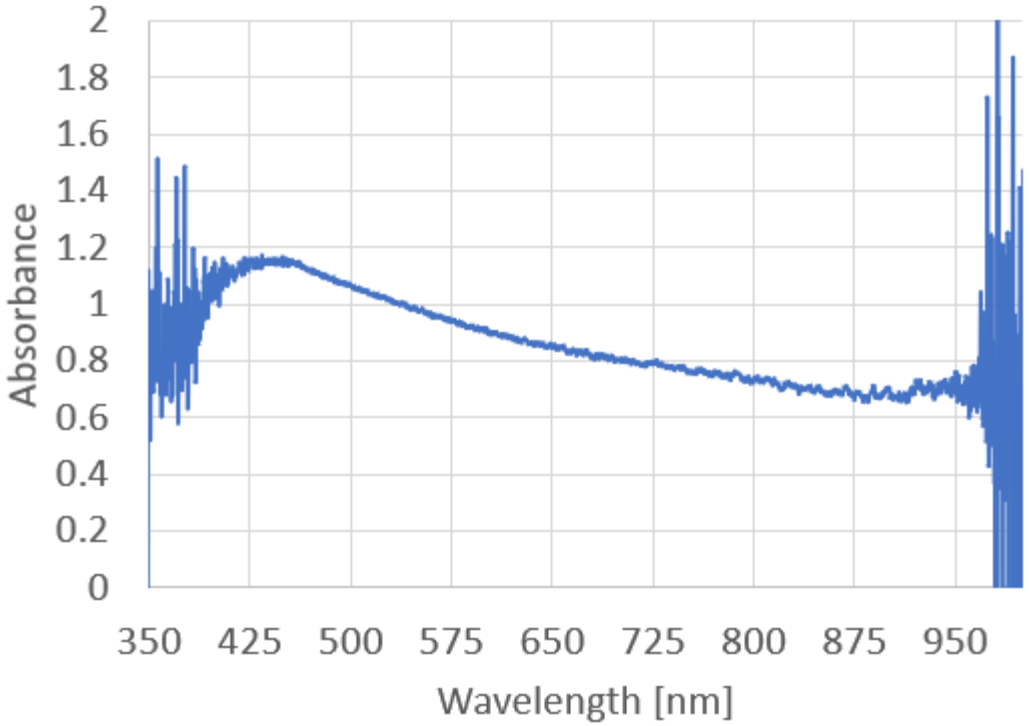

- $A = -\log_{10} T$
- Dissolved a small amount of $Ni(NO_3)\cdot 6H_2O$
- Absorbance peak appears near 425 nm, the expected location

Experimental Plans

- Complete benchmarking with nitrates and chlorides
- Move setup into glovebox
- Testing with purified FLiBe and controlled additions of corrosion products
- Testing with FLiBe samples from Karl's natural circulation loop

Acknowledgements and Questions

- Project funded by NEUP

- I’m happy to answer any questions!